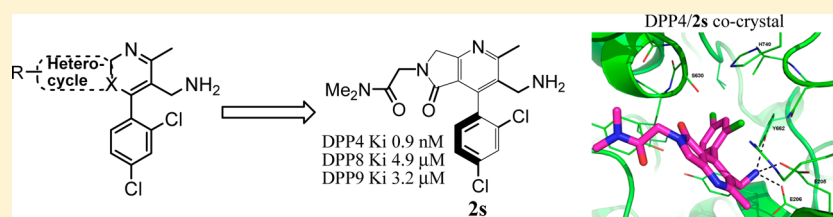


Optimization of Activity, Selectivity, and Liability Profiles in 5-Oxopyrrolopyridine DPP4 Inhibitors Leading to Clinical Candidate (*Sa*)-2-(3-(Aminomethyl)-4-(2,4-dichlorophenyl)-2-methyl-5-oxo-5*H*-pyrrolo[3,4-*b*]pyridin-6(7*H*)-yl)-*N,N*-dimethylacetamide (BMS-767778)

Pratik Devasthale,^{*,†} Ying Wang,[†] Wei Wang,[†] John Fevig,[†] JianXin Feng,[†] Aiyong Wang,[‡] Tom Harrity,[‡] Don Egan,[‡] Nathan Morgan,[‡] Michael Cap,[‡] Aberra Fura,[§] Herbert E. Klei,^{||} Kevin Kish,^{||} Carolyn Weigelt,[⊥] Lucy Sun,^{§,×} Paul Levesque,[§] Frederic Moulin,[§] Yi-Xin Li,[§] Robert Zahler,^{†,#} Mark S. Kirby,[‡] and Lawrence G. Hamann^{†,∞}

[†]Metabolic Diseases Chemistry, [‡]Metabolic Diseases Biology, [§]Pharmaceutical Candidate Optimization, ^{||}Protein Science and Structure, [⊥]Computer-Assisted Drug Design, Bristol-Myers Squibb Research and Development, Princeton, New Jersey 08543-5400, United States



ABSTRACT: Optimization of a 5-oxopyrrolopyridine series based upon structure–activity relationships (SARs) developed from our previous efforts on a number of related bicyclic series yielded compound **2s** (BMS-767778) with an overall activity, selectivity, efficacy, PK, and developability profile suitable for progression into the clinic. SAR in the series and characterization of **2s** are described.

INTRODUCTION

Dipeptidylpeptidase (DPP4) inhibitors,¹ such as sitagliptin,² saxagliptin,³ vildagliptin,⁴ and linagliptin,⁵ have emerged as a favorable class of agents constituting an effective therapeutic option in the treatment of diabetes mellitus, a debilitating condition that afflicts about 347 million people worldwide (WHO Fact Sheet No. 312, Sep 2012). This is due in part to their ability to control hyperglycemia alone or in combination with other agents and with reduced risk of hypoglycemia and weight gain, side effects that are common to several other oral antidiabetic therapies. During our efforts to identify backup candidates to saxagliptin, a number of novel chemotypes were discovered that less closely resemble substrate mimetic scaffolds.⁶ Compounds that were being evaluated in the clinic at the time had varied selectivities versus DPP8 and DPP9, the significance of which was unknown. A report⁷ from Merck on the potential liabilities of DPP8/9 inhibition using a DPP8/9-selective inhibitor in preclinical species suggested that it may be desirable to maximize selectivity versus DPP8 and DPP9. While a number of studies have subsequently suggested that inhibition of DPP8/9 is not associated with adverse events in humans, these data were not published at the time.^{7b–d} We decided to include selectivity as a criterion in our backup program to mitigate against any potential issues even if the significance of DPP selectivity was unclear. Additionally, a

greater placebo-subtracted HbA1c-lowering (>0.7 versus 0.4 that was achieved with 5 mg dose of saxagliptin) was observed in a 6-week phase II clinical trial with saxagliptin at 100 mg (unpublished data). However, because of potential concerns about using suprapharmacological doses, it was decided not to explore this dose in the clinic. It was therefore desirable to identify a potent, selective, and efficacious DPP4 inhibitor, optimally in a novel chemotype, with a high margin of safety to test the hypothesis in the clinic that greater HbA1c lowering could be achieved with continuous maximal DPP4 inhibition. This paper describes the culmination of those efforts with the identification of **2s** (BMS-767778), an optimized candidate from the 5-oxopyrrolopyridine series that was advanced into the clinic.

The design and rationale for arriving at a variety of substituted bicyclic scaffolds have been recently described^{6c,8a,8b} and are summarized in Figure 1. Earlier work from our laboratories^{6a–c} had identified the optimal point of attachment of the R group on a number of these scaffolds as indicated in Figure 1. X-ray structures from earlier series had suggested that this R group was exposed to solvent. The rationale for having a nitrogen atom on these bicyclic cores at this point of attachment was to allow facile

Received: June 17, 2013

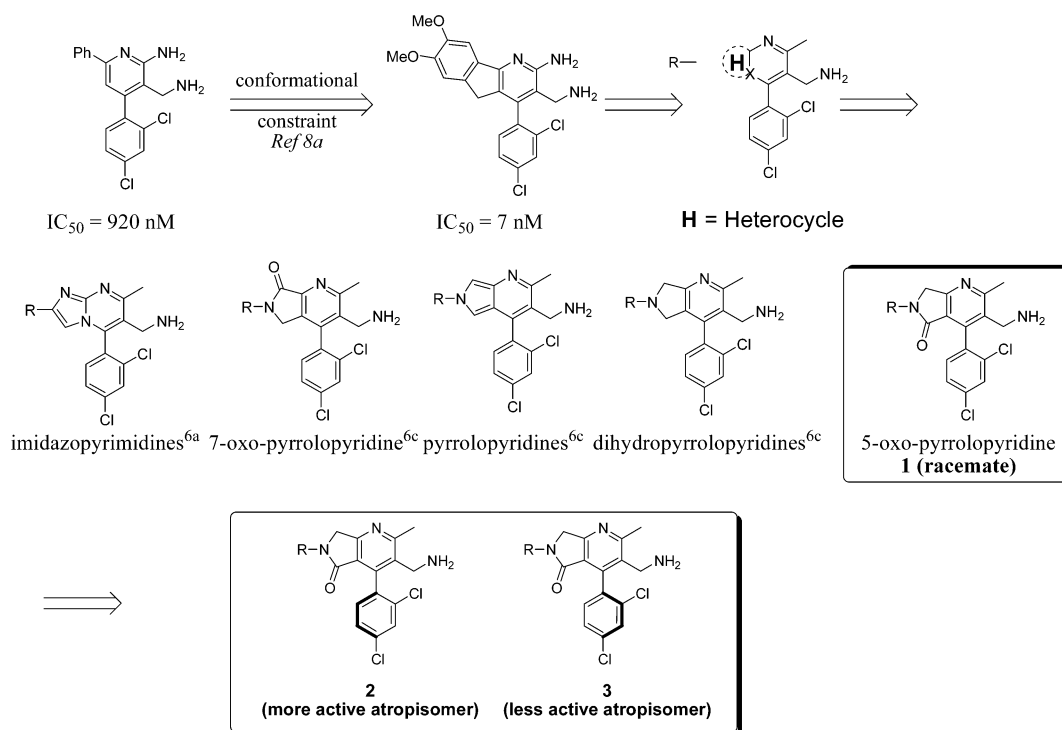


Figure 1. Design of novel bicyclic cores.

and rapid functionalization in this solvent-exposed region for optimization of activity and liability profiles.

Our previous X-ray analyses of compounds from multiple bicyclic series related to **1** had established that the more active atropisomer in every case was *Sa* with the 2-Cl atom in **2** pointing below the plane.^{6b–d} On the basis of previous work on closely related series in our group,^{6c,d} the 2,4-dichlorophenyl group was retained as an optimized aryl substitution at the 4-position of the pyridine.

RESULTS AND DISCUSSION

Schemes 1–4 outline the synthesis of 5-oxopyrrolopyridines with aryl, heteroaryl, and alkyl substituents on the lactam.

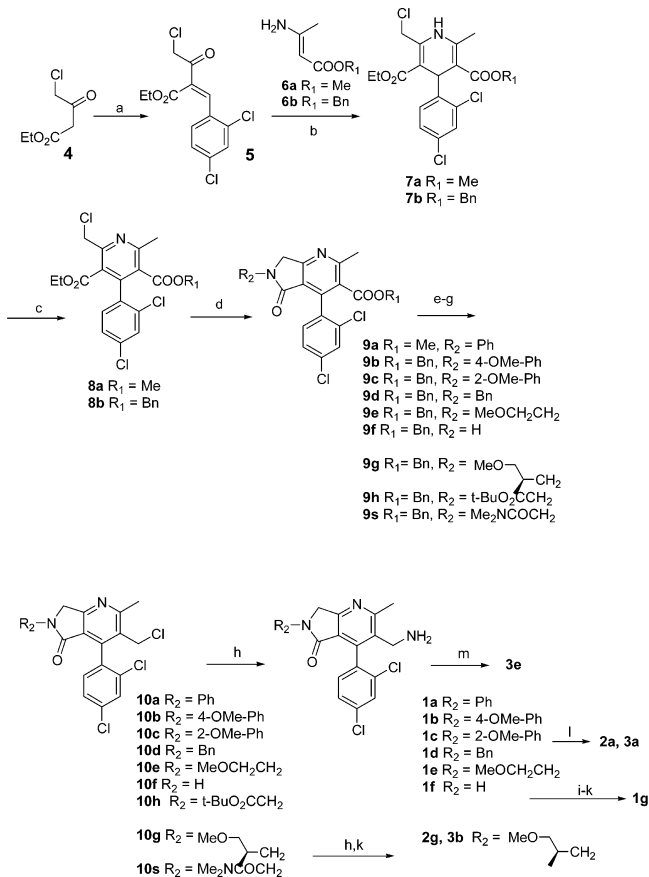
Dihydropyrrolopyridinones **1**, **2**, **3** could be prepared according to the general synthesis outlined in Scheme 1. Knoevenagel condensation of ethyl chloroacetate **4** with 2,4-dichlorobenzaldehyde gave styrene **5**. The dihydropyridyl ring was closed by further condensation of styrene **5** with enamine **6** to yield diester **7**. Oxidation of the dihydro species to the fully aromatic pyridine diester **8** was accomplished with nitric acid.⁹ Closure of the pyrrolidone ring by treatment with primary amine under microwave heating condition gave 5-oxopyrrolidinopyridine **9**. Debenzylation of **9b–g** and **9s** by hydrogenolysis or hydrolysis of methyl ester **9a** afforded the corresponding acid, which was subsequently reduced to primary alcohol via anhydride formed by treatment with ethyl chloroformate followed by reduction with NaBH₄. The alcohol was then converted into the corresponding chloride **10** by treatment with methanesulfonyl chloride. The desired primary amines **1**, **2**, and **3** were obtained by reaction of the chloride with NH₃/MeOH under microwave heating conditions. Homochiral analogues **3e**, **2a**, and **3a** were isolated by using chiral supercritical fluid chromatography (SFC) from the corresponding racemic precursors. The primary amine **1f** was protected with Boc₂O, and the resulting lactam was

converted into the carbamate via treatment with ClCO₂Et/Et₃N/DMAP followed by deprotection with TFA to afford **1g**.

The racemic intermediate **8b** was resolved to homochiral **11a** and **11b** using chiral supercritical fluid chromatography (SFC). Following the sequence described in Scheme 1, a number of homochiral analogues **2** and **3**, specified in Scheme 2, were synthesized using resolved atropisomeric intermediates **11a** and **11b**. Stereochemistry of intermediates **11a** and **11b** was assigned on the basis of inhibitory activities of pairs of enantiomers generated individually from **11a** and **11b**. The intermediate yielding the more active antipode was assigned the stereochemistry indicated in **11a**. In addition, in every case in this and other related bicyclic series for which we have X-ray cocrystal structure data (seven compounds from three different series 5-oxopyrrolopyridines, 7-oxopyrrolopyridines, and imidazopyrimidines), the more active atropisomer invariably had the *Sa* stereochemistry.

Scheme 3 describes the general synthesis of amide-containing 5-oxopyrrolopyridines. Debenzylation of **9i** by hydrogenolysis afforded acid **15**, which was subsequently reduced to the primary alcohol **16** via acid chloride prepared in situ with a combination of trichloroacetonitrile and triphenylphosphine¹⁰ followed by treatment with lithium tri-*tert*-butoxyaluminum hydride.¹¹ The racemate **16** was resolved by chiral supercritical fluid chromatography to give the desired atropisomer, which was converted to the corresponding chloride **17** by treatment with methanesulfonyl chloride. The acid **18** was obtained in an uneventful three-step sequence in 73% overall yield as shown in Scheme 3. Coupling of **18** with appropriate amines followed by deprotection yielded the target amides. The atropisomerically pure amino acid pair of **2l** and **3d** was derived from **10h** via conversion to the primary amine, chiral chromatographic separation, and deprotection.

An optimized, scalable protocol for the synthesis of **2s** is described in Scheme 4. Chloride **10s** was converted to the

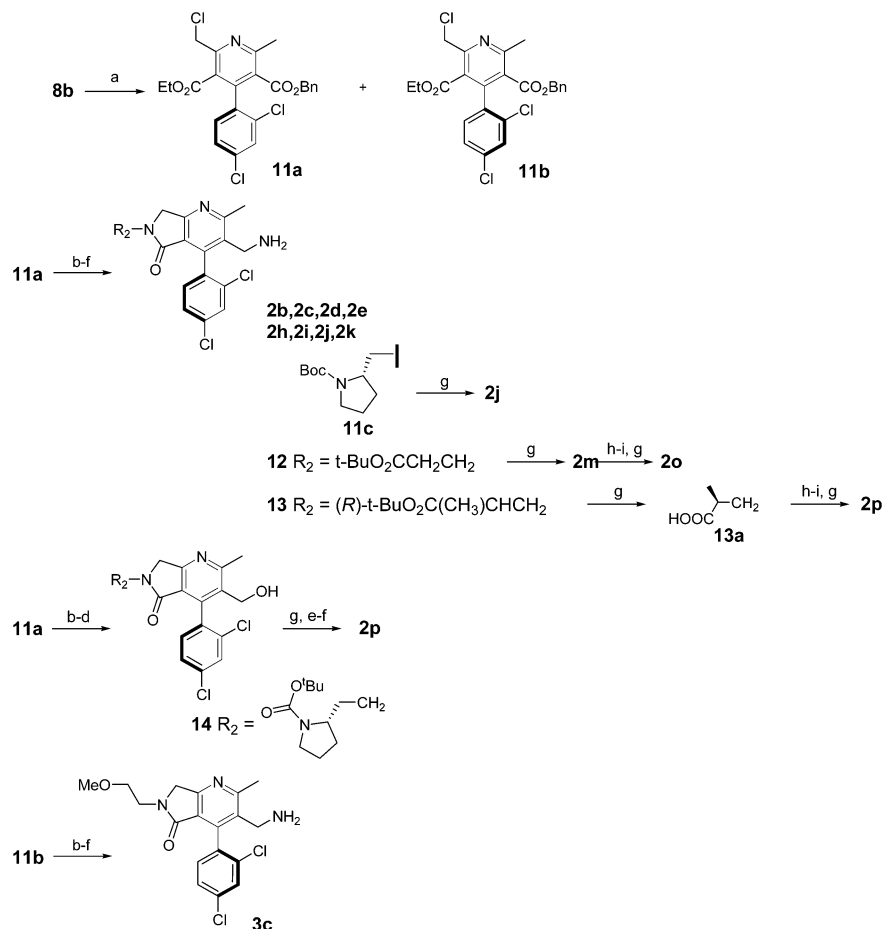
Scheme 1^a

^aReagents and conditions: (a) 2,4-dichlorobenzaldehyde, BnNH₂, AcOH, IPA, 100%; (b) IPA, 79% **7a**, 65% **7b**; (c) AcOH, HNO₃/H₂O, 57% **8a**, 68% **8b**; (d) R₂NH₂, EtOH, microwave 150 °C, 71% **9a**, 53% **9b**, 71% **9s**; (e) LiOH, THF, H₂O, 19% for **9a** or 10% Pd/C, H₂, EtOAc, 100% for **9b**–**s**; (f) ClCO₂Et, Et₃N, THF, then NaBH₄, THF, H₂O; (g) MsCl, Et₃N, CH₂Cl₂, 33% two steps **10a**, 7% two steps **10b**, 66% two steps **10s**; (h) 7 M NH₃ in MeOH, microwave 100 °C, 79% **1b**; (i) Boc₂O, NaHCO₃, THF; (j) ClCO₂Et, Et₃N, DMAP, CH₂Cl₂, 39% two steps; (k) TFA, CH₂Cl₂, 91% **1g**; (l) chiral separation (Chiralcel OJ 5 cm × 50 cm column; 20 μm; mobile phase, isocratic gradient of 15% EtOH–MeOH (50%) in heptane); (m) supercritical fluid chromatography (Chiralpak AD-H 250 mm × 30 mm i.d.; 5 μm; flow rate, 120 mL/min; mobile phase, CO₂/EtOH 75/25 with 0.1% DEA).

bis-Boc-protected amino intermediate **19** by treatment with KNBoc₂. The racemate **19** was resolved using SFC to obtain the desired atropisomeric intermediate **20**, which after removal of the Boc protecting groups under acidic conditions followed by basification afforded **2s** as a free base whose absolute stereochemistry was confirmed by X-ray analysis (Figure 2). In general, the stereochemistry of individual atropisomers was assigned on the basis of X-ray cocrystal structures of about a dozen analogues in the 5-oxo and multiple other bicyclic series.^{6b,c} The more active atropisomer was invariably significantly more potent than the less active atropisomer (for example, see **2f** vs **3c** and **2g** vs **3b** in Table 2 and **2l** vs **3d** in Table 3).

Analogous to our observations in the related 7-oxopyrrolopyridine series,^{6c} hERG, sodium channel, and CYP3A4 liabilities were evident in the 5-oxopyrrolopyridine series when the R group was aryl (Table 1). Mitigation of these liabilities was a major goal of the program. Additionally, though not clearly

demonstrated to be a significant issue, we also sought to mitigate against any potential concerns associated with DPP8/9 inhibition by maximizing DPP4 specificity. Ortho substitution on the phenyl group (**1c**) resulted in a 5-fold increase in potency at DPP4 and >1000-fold selectivity versus DPP8/9. X-ray structure analysis of the analogous homochiral 7-oxodihydropyrrolopyridinone (compound (+)-**3f** in ref 6c, PDB entry 3SX4) was consistent with two conformations of the ortho-methoxy group. In one orientation, the oxygen of the MeO group as well as the carbonyl oxygen of the 7-oxo group showed electrostatic interactions with Arg125. While an X-ray structure of **2a** is not available, one could speculate that a similar additional interaction with the ortho-MeO group may have contributed to the enhanced potency in the 5-oxo series as well. Essentially all phenyl- and benzyl-substituted analogues in Table 1 showed significant inhibition of CYP3A4. Introducing heteroaromatic groups to reduce clogP helped reduce the CYP3A4 liability to only a modest extent. For example, oxazole **2d**, with the lowest clogP in the table, showed an IC₅₀ against CYP3A4 of 8 μM. Alkyl-substituted analogues shown in Table 2, with the exception of **2k**, were relatively weaker inhibitors of CYP3A4. The hERG liability was greatly minimized by alkyl substitution (**1e**, **2g**, **3b**). Cyclic ethers (**2h**, **2i**) as well as basic groups (**2j**) were well-tolerated. However, the cyclic ethers were metabolically less stable while the pyrrolidine **2j** was about 10-fold less potent than our desired goal. The most potent DPP4 inhibitor from this series was **2k** with a K_i of 0.4 nM and DPP8/9 selectivity of 9500/7250, respectively. However, its IC₅₀ vs CYP3A4 of 3 μM and poor metabolic stability made it nonprogressible. A significant finding was that the unsubstituted lactam **1f** retained modest DPP4 inhibitory activity and good DPP8/9 selectivity and had minimal hERG and CYP3A4 liabilities (Table 3). The goal at this point was to improve upon its DPP4 potency while retaining the beneficial overall profile. Previous SAR findings in our group as well as examination of several X-ray cocrystal structures of earlier analogous compounds had suggested that the substituent on the lactam nitrogen was exposed to solvent and hence an optimal position to explore functionalities that would potentially retain DPP4 activity and selectivity versus DPP8/9 and mitigate hERG and CYP3A4 liabilities. We were pleased to find that homochiral acids such as **2l** and **2m** and homochiral amides such as **2n**, **2o**, and **2p**, which lent themselves to facile SAR exploration, exhibited potent DPP4 inhibition. While the acids showed superior CYP3A4 profiles compared with the amides, they were also generally more potent at DPP9 (for example, **2m**, K_i = 300 nM). On the other hand, amides had K_i values of 7–10 μM against CYP3A4. The most potent compound from Table 3, **2n**, suffered from poor metabolic stability in mouse liver microsomes. However, the finding triggered a concerted search, driven by structure–activity and structure–liability data analysis, for an optimal amide substituent with a superior profile. None of the compounds in Table 4 displayed any hERG flux activity up to 80 μM. In general, lactam substituents containing a free acid, nitrogen-containing basic groups, and primary and secondary amide groups showed poor PAMPA permeability (data not shown). PAMPA permeability at pH 7.4 for most neutral aliphatic and aromatic substituents as well as for tertiary amides was high. Further optimization of the amide functionality (Table 4) yielded compound **2s** with an overall profile that was suitable for progression into efficacy studies. Other close analogues that were of comparable potency, selectivity, and CYP3A4 profile to **2s** had inferior metabolic stability or poor permeability. For example, **2r** had a PAMPA permeability of 87 nm/s at pH 7.4

Scheme 2^a

^aReagents and conditions: (a) supercritical fluid chromatography (Chiralpak AD 250 mm × 4.6 mm i.d.; 10 μm; 35 °C; flow rate, 2.0 mL/min; mobile phase, CO₂/IPA 82/18; injection volume, 5 μL; detector wavelength, 220 nm); (b) R₂NH₂, EtOH, microwave 150 °C; (c) 10% Pd/C, H₂, EtOAc, 100%; (d) ClCO₂Et, Et₃N, THF, then NaBH₄, THF, H₂O; (e) MsCl, Et₃N, CH₂Cl₂; (f) 7 M NH₃ in MeOH, microwave 100 °C; (g) TFA, CH₂Cl₂, 46%; (h) Boc₂O, NaHCO₃, THF, H₂O; (i) Et₂NH, PyBOP, DIEA, THF, 100% two steps.

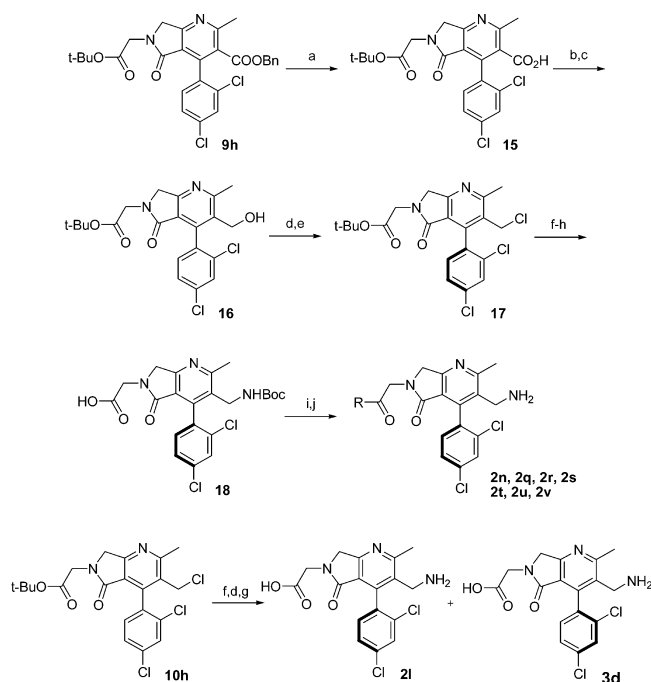
versus 330 nm/s for **2s**. Compound **2t**, while more potent and comparably selective versus DPP8/9, had a worse CYP3A4 and metabolic stability profile than **2s**. The more active atropisomer **2s**, with the *S* stereochemistry (confirmed by X-ray analysis, Figure 2), was 14-fold more potent than the less active atropisomer **3e** at inhibiting DPP4 and also showed a bigger therapeutic window versus CYP3A4. Compound **2s** had a DPP4 *K*_i of 0.9 nM and a DPP8/9 selectivity of 5400 and 3600, respectively. The atropisomeric integrity was unchanged after incubation of **2s** in human and rat plasma for 3 h at 37 °C.

Compound **2s** was further characterized by cocrystallization within the active site of DPP4 (Figure 2).^{12a} As with previous X-ray structures resolved for earlier analogues within this chemotype, the dominant nonhydrophobic interactions were between the basic primary amine of **2s** and the two glutamate residues E206/E207 of DPP4. As was observed in the 7-oxo series,^{6c} the amide functionality on the lactam was exposed to solvent. There were no interactions detected with the catalytic Ser630. The amide carbonyl appeared to have a stacking interaction with Tyr547, which may have contributed to DPP4 potency. Similar π–π interactions were observed in X-ray structures of phenyl-substituted lactams as well. Overall, there were fewer interactions in the S630-containing α/β-hydrolase domain relative to saxagliptin,^{12b} consistent with the hypothesis

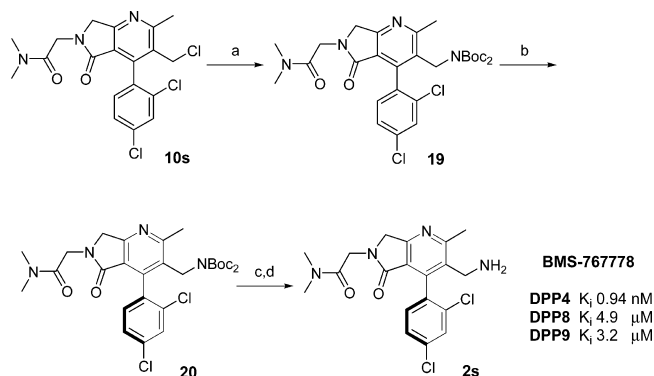
that greater selectivity could be achieved by taking advantage of a lower homology among DPP members in the β-propeller domain.

The permeability (*P*_c) in the PAMPA model was pH-dependent and, at pH ≥ 6.5 (typical pH range in human intestine), was similar to *P*_c values of compounds that exhibit good (>80%) absorption in humans (Table 5). The basolateral-to-apical permeability of **2s** was ≥5-fold higher versus apical-to-basolateral permeability in Caco-2 cells (pH ≥ 6.5; data shown are at pH 7.4), suggesting that it is a substrate of efflux transporters. The percent of **2s** bound to serum proteins was low in all species tested. The rate of **2s** metabolism in vitro (liver microsomes and hepatocytes) was low to moderate, and a low hepatic clearance in humans was predicted. In vivo, the total blood clearance of **2s** was low to intermediate in rats, dogs, and monkeys but high in mice (Table 6). Overall, the elimination of **2s** appeared to be mediated by both hepatic metabolism and renal excretion, with a minor contribution from biliary excretion. Compound **2s** had a favorable pharmacokinetic profile and good absorption properties with an absolute oral bioavailability ranging from 41% to 95% across animal species.

Oral Glucose Tolerance in ob/ob Mice. On the basis of its in vitro potency, selectivity, PK, and a favorable profile in in vitro liability assays, compound **2s** was selected for detailed evaluation

Scheme 3^a

^aReagents and conditions: (a) H₂, 10% Pd/C, 100%; (b) CCl₃CN, Ph₃P resin, CH₂Cl₂; (c) LiAl(OBu)₃H, THF, 0 °C, 80% two steps; (d) supercritical fluid chromatography (Chiralpak AD 250 mm × 4.6 mm i.d.; 10 μm; 35 °C; flow rate, 2.0 mL/min; mobile phase, CO₂/IPA 82/18; injection volume, 5 μL; detector wavelength, 220 nm); (e) MsCl, Et₃N, CH₂Cl₂, 0 °C, >90%; (f) 7 M NH₃ in MeOH, 50 °C; (g) TFA, CH₂Cl₂; (h) Boc₂O, NaHCO₃, THF, H₂O, 73% three steps; (i) HOBt·H₂O, EDCI, NH₄Cl, DIEA, DMF, 2q; amine, PyBOP, DIEA, THF, 2n, 2r, 2s, 2t, 2u, 2v; (j) TFA, CH₂Cl₂, 12–74% two steps.

Scheme 4^a

^aReagents and conditions: (a) KNBoc₂, THF/DMF (15:5), 60 °C, 60%; (b) supercritical fluid chromatography (Chiralpak AD 250 mm × 4.6 mm i.d.; 10 μm; 35 °C; flow rate, 2.0 mL/min; mobile phase, CO₂/IPA 82/18; injection volume, 5 μL; detector wavelength, 220 nm); (c) 4 N HCl, dioxane; (d) 1 N NaOH, CH₂Cl₂, 86% two steps.

in vivo models of efficacy and safety. When tested in vivo in insulin resistant high fat fed (HFD) ob/ob mice, which were given an oral glucose tolerance test (oGTT) 1 or 4 h after dose, 2s demonstrated an insulinotropic effect at all doses, with insulin AUCs increasing 2-, 3.8-, 2.5-, and 3.1-fold over the vehicle response at the 0.3, 1, 3, and 10 μmol/kg dose levels, respectively (Figure 3). The 0.3 and 3 μmol/kg dose treatment groups did not achieve statistical significance in this study. In a separate

mouse PK study, C_{max} and T_{max} for 2s were determined to be 56 nM and 1 h after an oral dose of 0.82 mpk, respectively. With a mouse plasma free fraction of 14%, coverage over DPP4 K_i would be expected during the efficacy study.

These effects on insulin translated into decreases in peak glucose concentrations (Figure 4). All doses of 2s above 0.3 μmol/kg gave maximal decreases in peak glucose, similar to that seen with the 3 μmol/kg dose of BMS-538305.¹³

The selection of 2s as the clinical candidate was arrived at after an extensive analysis of all available in vitro and in vivo activity and liability data for advanced leads from multiple distinct chemotypes. In particular, differentiating areas among advanced leads pertained to metabolism, reactive intermediate formation, pharmacokinetic properties, and overall target potency. A desirable profile of the candidate included having a DPP4 potency comparable to that of saxagliptin (~1 nM) and in vitro selectivity ratios versus DPP8/9 that were significantly higher than those for saxagliptin. Although the 7-oxopyrrolidinone series described earlier^{6c} was the most potent series with K_i values for leads in the 300–600 pM range, the series suffered from the poorest pharmacokinetic properties and was therefore not advanced. In the imidazopyrimidine^{6a,b} and the 5-oxopyrrolidinone series, a number of compounds showed evidence of mild time-dependent CYP3A4 inhibition. After analysis of over 100 analogues in this assay, candidates were advanced on the basis of a lack of time dependency and weakest overall inhibition potency. Additionally, several analogues showed evidence of reactive intermediate formation in glutathione trapping studies, presumably through the intermediacy of an oxime group arising from the benzylamine functionality. Only compounds that showed acceptable profiles in this reactive intermediate assays were advanced further. Further detailed comparative analysis of the full profiles of the best leads from each series resulted in the selection of 2s as a candidate for toxicological evaluation in cynomolgous monkeys, where 2s was determined to be acceptable for advancement to the clinic.

The toxicology profile of 2s was evaluated in a battery of in vitro safety tests as well as in vivo tests in rats and dogs. No adverse effects were identified after single (up to 500 mg/kg) or repeated (up to 300 mg/kg) oral dosing for up to 14 days in rats. No clinical chemistry or hematology changes were seen with 2s. In the dog, administration of 2s once daily for 5 days produced no significant dose-related changes at doses up to 25 mg/kg. At 50 mg/kg, a softening of stools was noted. Compound 2s did not demonstrate any potential for undesirable cardiovascular activity at an oral dose of 50 mg/kg. On the basis of the results of human in vitro assays and allometrically scaled animal data, 2s was predicted to be a low clearance compound in human with a projected human efficacious dose of 13–33 mg q.d. Because of the absence of any significant dose-limiting toxicities in preclinical toxicology studies, 2s was considered to have demonstrated an overall efficacy, safety, and developability profile suitable for advancement to the clinic, allowing for exploring a hypothesis that higher sustained exposures above what are required for maximal DPP4 inhibition of a potent and selective DPP4 inhibitor with an acceptable safety margin would achieve greater HbA1c reductions in humans.

EXPERIMENTAL SECTION

All reactions were carried out under a static atmosphere of argon or nitrogen, and mixtures were stirred magnetically unless otherwise noted. All reagents used were of commercial quality and were obtained from Aldrich Chemical Co., Sigma Chemical Co., Lancaster Chemical Co.,

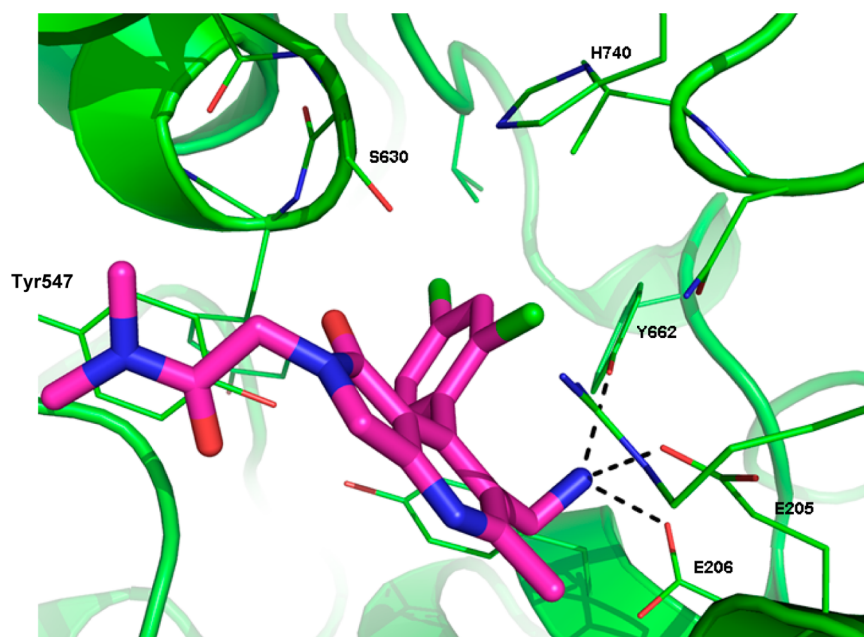


Figure 2. X-ray cocrystal structure of 2s bound to the DPP4 active site at 2.35 Å resolution.

Table 1. *N*-Aryl- and *N*-Benzyl-5-oxopyrrolopyridines

Comp	R	Chemical Structure			hERG EP %Inh @ 10 μM	CYP-3A4 ^b IC ₅₀ (μM)	Mouse Met. Stab. % remaining ^d	clogP
		1 (racemate)	2 (more active atropisomer)	3 (less active atropisomer)				
1a		21	5.2/3.4	50	ND ^c	ND	4.2	
1b		20	2.8/1.3	43	0.9	ND	4.2	
1c		3.9 ± 0.79	3.9/5.4	38	0.8	61	4.2	
2a		1.9 ± 0.52	3.8/2.3	51	3.4	67	4.2	
3a		63	>30/>30	ND	0.8	64	4.2	
2b		11	5.5/1.2	ND	11	72	2.4	
1d		29	6.4/>10	ND	0.9	48	3.8	
2c		3.4	5.2/3.7	ND	7.9	54	1.9	
2d		2.6	8.9/7.3	37	7.7	94	1.5	
2e		2.3	6.0/4.3	ND	4.7	63	2.0	

^a*n* = 1–3. ^bVersus substrate 7-benzyloxy-4-trifluoromethyl coumarin. ^cND = not determined. ^dIncubation in mouse liver microsomes for 10 min at 3 μM compound and 1 mg/mL protein.

or Acros Chemical Co. ¹H (400 MHz) and ¹³C (100 MHz) NMR spectra were recorded on a JEOL GSX400 spectrometer using Me₄Si as

an internal standard unless otherwise noted. ¹H (500 MHz) and ¹³C (125 MHz) NMR spectra were recorded on a JEOL JNM-ECP500

Table 2. *N*-Alkyl-5-oxopyrrolopyridines

Comp	R	DPP4 Ki (nM) ^a	DPP8/9 Ki (μM) ^a	hERG EP %Inh @ 10 μM	CYP-3A4 ^b IC ₅₀ (μM)	Mouse Met. Stab. % remaining ^d
1e (BMS-744891)		8.3	7.1/4.6	10	23	74
2f		6.0	5.4/1.9	ND ^c	29	65
3c		160	>30/>30	ND	14	69
2g		7.4	1.7/2.3	11	13	43
3b		31	>30/>30	8	13	24
2h		2.7 ± 0.27	3.9/3.1	ND	14	37
2i		1.0 ± 0.26	1.4/0.5	ND	15	50
2j		7.5	>30/>30	ND	40	100
2k		0.4	3.8/2.9	ND	3.0	36

^a*n* = 1–3. ^bVersus substrate 7-benzyloxy-4-trifluoromethyl coumarin. ^cND = not determined. ^dIncubation in mouse liver microsomes for 10 min at 3 μM compound and 1 mg/mL protein.

Table 3. Acid-, Ester-, and Amide-Containing 5-Oxopyrrolopyridines

Comp	R	DPP4 Ki (nM) ^a	DPP8/9 Ki (μM) ^a	hERG EP %Inh @ 10 μM	CYP-3A4 ^b IC ₅₀ (μM)	Mouse Met. Stab. % remaining ^d
1f	H	14	>30/>30	16	>40	99
1g		30	>30/>30	15	6.4	59
2l		1.7	2.5/0.9	ND ^c	>40	failed
3d		11	1.0/>30	ND	ND	ND
2m		1.0	1.8/0.3	ND	>40	failed
2n		0.3	0.8/1.3	5	6.6	50
2o		6.6	3.9/2.8	ND	8.3	5
2p		2.5	3.8/6.8	ND	9.6	0

^a*n* = 1–3. ^bVersus substrate 7-benzyloxy-4-trifluoromethyl coumarin. ^cND = not determined. ^dIncubation in mouse liver microsomes for 10 min at 3 μM compound and 1 mg/mL protein.

spectrometer. Chemical shifts are given in parts per million (ppm) downfield from internal reference Me₄Si in δ units, and coupling constants (*J*) are given in hertz (Hz). Selected data are reported in the following manner: chemical shift, multiplicity, coupling constants. All reactions were carried out using commercially available anhydrous

solvents from Aldrich Chemical Co. or EM Science Chemical Co. unless otherwise noted. All flash chromatographic separations were performed using E. Merck silica gel (particle size, 0.040–0.063 mm). Reactions were monitored by TLC using 0.25 mm E. Merck silica gel plates (60 F₂₅₄) and were visualized with UV light, with 5% phosphomolybdic

Table 4. Acetamide-Substituted 5-Oxopyrrolopyridines

Comp	R	DPP4 Ki (nM) ^a	DPP8/9 Ki (μM) ^a	CYP-3A4 ^b IC ₅₀ (μM)	clogP	Mouse Met. Stab. % remaining ^c
2q		4.2	13/5.4	>40	1.0	100
2r		2.1 ± 0.34	4.3/3.3	>40	1.3	95
2s (BMS-767778)		0.94 ± 0.18	4.9/3.2	36	1.7	93
3e		13.0	>30.0/>30.0	13	1.7	100
2t		0.4	2.0/1.8	5.5	2.8	53
2u		0.4	1.4/0.9	23	2.0	73
2v		0.8	1.0/0.8	8.2	2.6	45

^a*n* = 1–3, except for 2s (*n* = 32). ^bVersus substrate 7-benzyloxy-4-trifluoromethylcoumarin. ^cIncubation in mouse liver microsomes for 10 min at 3 μM compound and 1 mg/mL protein.

Table 5. Permeability and Plasma Protein Binding Profile of 2s

<i>P_o</i> , nm/s (PAMPA) (<i>n</i> = 3)	
pH 5.5	19.7 ± 3.8
pH 6.5	129.7 ± 12.9
pH 7.4	330 ± 49
<i>P_o</i> , nm/s (Caco-2) ^a	
apical to basolateral	26 ± 1
basolateral to apical	131 ± 18
plasma protein binding, % free	
human	18
mouse	14
rat	28
dog	27
monkey	16

^aMeasured at pH 7.4.

Table 6. Pharmacokinetic Profile of 2s^a

	mouse	rat	dog	monkey
iv dose (mg/kg)	0.82	0.82	3	3
po dose (mg/kg)	0.82	0.82	3	3
CL (mL min ⁻¹ kg ⁻¹)	137	40.9	10.6	19.2
<i>V_{ss}</i> (L/kg)	6.3	2.9	2.7	2.8
<i>T</i> _{1/2} (h)	1.8	1.5	7.8	5.6
bioavailability (%)	41	48	95	84

^aVehicle used in iv and po studies in all species: water.

acid in 95% EtOH or by a sequential treatment with 1 N HCl/MeOH followed by ninhydrin staining. LC/MS data were recorded on a Shimadzu LC-10AT equipped with a SIL-10A injector, a SPD-10AV detector normally operating at 220 nm, and interfaced with a Micromass ZMD mass spectrometer. HPLC retention times, unless otherwise noted, are reported using a Zorbax SB C18 4.6 mm × 75 mm column. The gradient solvent system was from 100% A/0% B to 0% A/100% B (A = 90% H₂O/10% MeOH + 0.2% H₃PO₄) (B = 90% MeOH/10% H₂O + 0.2% H₃PO₄) for 8 min. Detection was at 220 nm. All solvents

were removed by rotary evaporation under vacuum using a standard rotovap equipped with a dry ice condenser. All filtrations were performed with a vacuum unless otherwise noted. All final compounds were purified to >95% purity by HPLC analysis.

(Z)-Ethyl 4-Chloro-2-(2,4-dichlorobenzylidene)-3-oxobutanoate (5). A solution 2,4-dichlorobenzaldehyde (4.6 g, 26.1 mmol), ethyl 4-chloro-3-oxobutanoate (4.5 g, 27.4 mmol), benzylamine (165 mg, 1.5 mmol), and acetic acid (118 mg, 2.0 mmol) in isopropyl alcohol (30 mL) was stirred at ambient temperature for 96 h. The mixture was diluted with isopropyl alcohol to give a total volume of 50 mL and was saved as a stock solution (0.52 mmol/mL).

(E)-Benzyl 3-Aminobut-2-enoate (6b). A mixture of benzyl acetate 4.6 g, 24 mmol) and ammonium acetate (9.2 g, 119.5 mmol) in methanol (30 mL) was allowed to stir at ambient temperature for 72 h. The solvent was evaporated, and the residue was taken up in CHCl₃/H₂O. The combined organic layer was washed with brine, dried (Na₂SO₄), and evaporated to give 6b (4.3 g, 90% yield) as a golden oil. ¹H NMR (400 MHz, CDCl₃) δ 9.1 (s, 3H), 4.60 (s, 1H), 5.12 (s, 2H), 7.24–7.40 (m, 5H).

Ethyl 2-(Chloromethyl)-4-(2,4-dichlorophenyl)-5-(2-methoxy-2-oxoethyl)-6-methyl-1,4-dihydropyridine-3-carboxylate (7a). A mixture of 2,4-dichlorobenzaldehyde (2.3 g, 12.9 mmol), ethyl 4-chloro-3-oxobutanoate (2.2 g, 12.9 mmol), benzylamine (80.0 mg, 0.8 mmol), and acetic acid (55.0 mg, 0.9 mmol) in isopropyl alcohol (15 mL) was stirred at ambient temperature for 65 h. 6a (1.6 g, 14.4 mmol) was added to the reaction mixture, and stirring continued at ambient temperature for 24 h. The reaction was quenched with concentrated HCl (1 mL), and the mixture was stirred at ambient temperature for 2 h. The reaction mixture was then concentrated in vacuo, diluted with diethyl ether, filtered, and evaporated. The residue was purified by flash chromatography (120 g column, 0–100% EtOAc/hexanes) to yield 7a (4.2 g, 79% yield) as a yellow sticky oil. ¹H NMR (400 MHz, CDCl₃) δ 1.22 (t, *J* = 7.5 Hz, 3H), 2.36 (s, 3H), 3.63 (s, 3H), 4.11 (q, *J* = 7.2 Hz, 2H), 4.86 and 4.97 (AB_q, *J* = 14.0 Hz, 2H), 5.40 (s, 1H), 6.40 (broad s, 1H), 7.13 (dd, *J* = 8.4, 2.2 Hz, 1H), 7.26–7.31 (m, 2H). *m/z* = 418 [M + H]⁺.

3-Benzyl 5-Ethyl 6-(chloromethyl)-4-(2,4-dichlorophenyl)-2-methyl-1,4-dihydropyridine-3,5-dicarboxylate (7b). A mixture of stock solution 5 (25 mL, 13 mmol) and 6b (2.8 g, 14.5 mmol) in isopropyl alcohol (3 mL) was allowed to stir at ambient temperature for 18 h. The reaction was quenched with concentrated HCl (8 mL), and the mixture was stirred at ambient temperature for 2 h. The mixture was concentrated in vacuo, diluted with diethyl ether, filtered, and

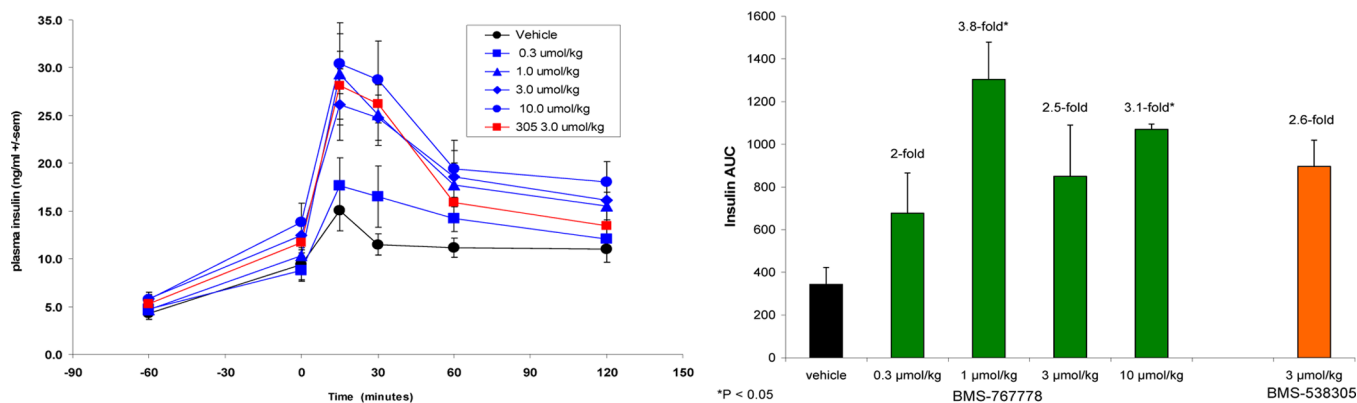


Figure 3. Insulin response and effects on plasma insulin AUC during an oGTT in an ob/ob mouse model, following treatment with **2s**.

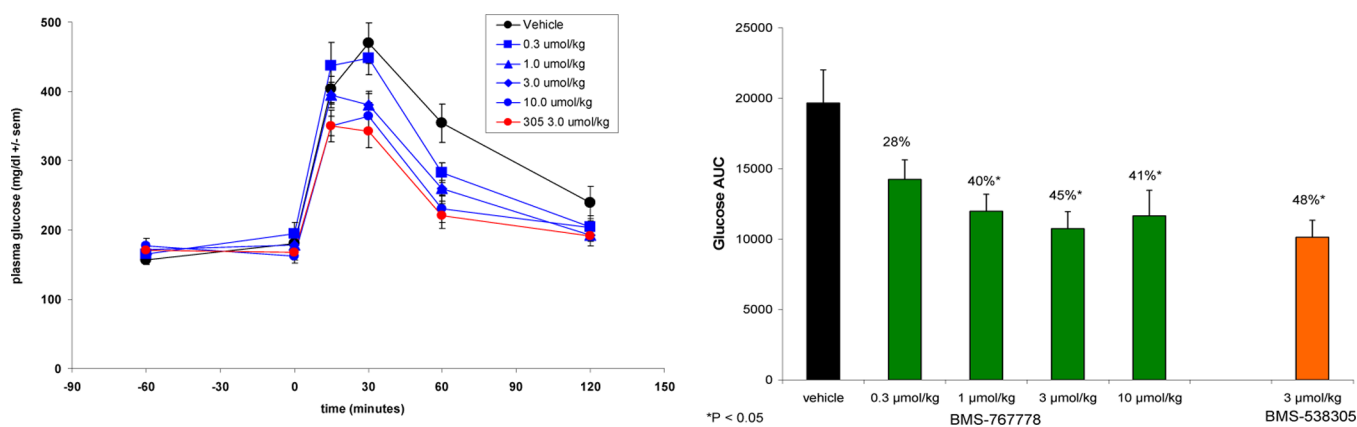


Figure 4. Glucose response and effects on glucose AUC during an oGTT in an ob/ob mouse model, following treatment with **2s**.

evaporated. The residue was purified by flash chromatography (120 g column, EtOAc/hexanes) to give **7b** (4.2 g, 65% yield) as a yellow sticky oil. $^1\text{H NMR}$ (400 MHz, CDCl_3) δ 1.19 (t, $J = 7.0$ Hz, 3H), 2.35 (s, 3H), 4.05–4.15 (m, 2H), 4.82 and 4.97 (AB_q, $J = 14.1$ Hz, 2H), 5.07 and 5.11 (AB_q, $J = 12.3$ Hz, 2H), 5.41 (s, 1H), 6.37 (broad s, 1H), 7.07 (dd, $J = 8.4$, 2.2 Hz, 1H), 7.16–7.32 (m, 5H), 7.35–7.38 (m, 2H).

3-Ethyl 5-Methyl 2-(chloromethyl)-4-(2,4-dichlorophenyl)-6-methylpyridine-3,5-dicarboxylate (8a). **7a** (3.4 g, 8.1 mmol) was dissolved in acetic acid (15 mL) and 70% nitric acid/water (15 mL). The reaction mixture was stirred at ambient temperature for 72 h. The crude product (3.7 g) was purified by flash chromatography (120 g column, 0–100% EtOAc/hexanes) to give **8a** (1.9 g, 57% yield) as a pale yellow oil. $^1\text{H NMR}$ (400 MHz, CDCl_3) δ 1.02 (t, $J = 7.7$ Hz, 3H), 2.66 (s, 3H), 3.60 (s, 3H), 4.10 (q, $J = 7.0$ Hz, 2H), 4.80 and 4.93 (AB_q, $J = 11.0$ Hz, 2H), 7.13 (d, $J = 7.0$ Hz, 1H), 7.26–7.33 (m, 1H), 7.45 (s, 1H). $m/z = 416$ [M + H]⁺.

3-Benzyl 5-Ethyl 6-(chloromethyl)-4-(2,4-dichlorophenyl)-2-methylpyridine-3,5-dicarboxylate (8b). **7b** (4.1 mg, 8.2 mmol) was dissolved in acetic acid (30 mL) and 70% nitric acid/water (25 mL). The reaction mixture was allowed to stir at ambient temperature for 18 h. The crude product (4.2 g) was purified by flash chromatography (120 g column, 0–100% EtOAc/hexanes) to give **8b** (2.7 g, 68% yield) as a pale yellow oil. $^1\text{H NMR}$ (400 MHz, CDCl_3) δ 0.98 (t, $J = 7.3$ Hz, 3H), 2.65 (s, 3H), 4.05 (q, $J = 7.0$ Hz, 2H), 4.77 and 4.92 (AB_q, $J = 11.0$ Hz, 2H), 5.04 (s, 2H), 7.01 (d, $J = 8.35$ Hz, 1H), 7.07 (dd, $J = 8.4$, 2.2 Hz, 1H), 7.10–7.14 (m, 2H), 7.21 (d, $J = 2.2$ Hz, 1H), 7.28–7.28 (m, 3H). $m/z = 492$ [M + H]⁺.

(S)-3-Benzyl 5-Ethyl 6-(chloromethyl)-4-(2,4-dichlorophenyl)-2-methylpyridine-3,5-dicarboxylate (11a) and (R)-3-Benzyl 5-Ethyl 6-(chloromethyl)-4-(2,4-dichlorophenyl)-2-methylpyridine-3,5-dicarboxylate (11b). **8b** was separated into individual atropisomers using supercritical fluid chromatography (SFC). Conditions: Whelk O-1 SS, 500 mm × 20 mm, 10 μm ; 35 °C; 5% IPA with 0.1% DEA in SFC-CO₂; 100 bar; 60 mL/min; 220 nm. Faster-eluting isomer: **11a**.

$[\alpha]_{\text{D}}^{25} +54.45^\circ$ (*c* 10.21 mg/mL, CHCl_3). Analytical HPLC: gradient solvent system from 100% A/0% B to 0% A/100% B (A = 90% H₂O/10% MeOH + 0.2% H₃PO₄) (B = 90% MeOH/10% H₂O + 0.2% H₃PO₄) for 4 min; detection at 220 nm. YMC SS ODS Ballistic 4.6 mm × 50 mm column; $t_{\text{R}} = 4.8$ min. Chiral analytical HPLC: $t_{\text{R}} = 7.39$ min on analytical SFC [Regis (S,S) Whelk-OI 250 mm × 4.6 mm i.d.; 10 μm (S/N 200036); mobile phase CO₂/IPA, 95/5; flow rate, 2.0 mL/min]. Slower-eluting isomer: **11b**. $[\alpha]_{\text{D}}^{25} -52.87^\circ$ (*c* 1.021, CHCl_3). $t_{\text{R}} = 7.92$ min on chiral analytical SFC.

Methyl 4-(2,4-Dichlorophenyl)-2,7-dimethyl-5-oxo-6-phenyl-6,7-dihydro-5H-pyrrolo[3,4-*b*]pyridine-3-carboxylate (9a). A mixture of **8a** (671 mg, 1.6 mmol) and aniline (168 mg, 1.8 mmol) in ethanol (5 mL) was heated to 175 °C for 45 min in a microwave reactor. The mixture was purified by flash chromatography (120 g column, 0–100% EtOAc/hexanes) to give **9a** (485 mg, 71% yield) as a pale brown solid. $^1\text{H NMR}$ (400 MHz, CDCl_3) δ 2.77 (s, 3H), 3.64 (s, 3H), 4.88 and 5.00 (AB_q, $J = 17.6$ Hz, 2H), 7.13–7.20 (m, 2H), 7.33 (dd, $J = 8.4$, 2.2 Hz, 1H), 7.36–7.44 (m, 2H), 7.53 (d, $J = 1.8$ Hz, 1H), 7.79 (d, $J = 7.9$ Hz, 2H). $m/z = 473$ [M + H]⁺.

Benzyl 4-(2,4-Dichlorophenyl)-6-(4-methoxyphenyl)-2-methyl-5-oxo-6,7-dihydro-5H-pyrrolo[3,4-*b*]pyridine-3-carboxylate (9b). A mixture of **8b** (199 mg, 0.4 mmol) and 4-methoxybenzylamine (61 mg, 0.5 mmol) in ethanol (3 mL) was heated in a microwave reactor at 175 °C for 15 min. The solvent was evaporated and the residue was purified by flash chromatography (12 g column, EtOAc/hexanes) to give **9b** (114.6 mg, 53% yield) as a golden oil. $^1\text{H NMR}$ (400 MHz, CDCl_3) δ 2.76 (s, 3H), 3.79 (s, 3H), 4.81 and 4.90 (AB_q, $J = 17.6$ Hz, 2H), 5.05 and 5.11 (AB_q, $J = 11.9$ Hz, 2H), 6.89 (d, $J = 9.2$ Hz, 2H), 7.03 (d, $J = 8.4$ Hz, 1H), 7.08–7.16 (m, 3H), 7.28–7.38 (m, 4H), 7.66 (d, $J = 9.2$ Hz, 2H). $m/z = 533$ [M + H]⁺.

Benzyl 4-(2,4-Dichlorophenyl)-6-(2-(dimethylamino)-2-oxoethyl)-2-methyl-5-oxo-6,7-dihydro-5H-pyrrolo[3,4-*b*]pyridine-3-carboxylate (9s). **8b** (72.0 g, 0.146 mol) was dissolved in dimethylacetamide (130 mL). This solution was added in three portions

as described below. To a mixture of glycine dimethylamide hydrochloride salt (25.9 g, 0.187 mol) in dimethylacetamide (150 mL) at room temperature was added triethylamine (122.5 mL, 0.879 mol). The resulting slurry was heated at 80 °C. The solution of chloride **8b** in DMA (60 mL) as previously described was added over a period of 10 min. The resultant mixture was stirred for an additional 50 min period. A second portion of the chloride solution (60 mL) was added over a period of 10 min. The mixture was then stirred at this temperature for 1.5 h. The remainder of the chloride solution was added over a period of 10 min, and the resulting mixture was stirred for an additional 2 h. After the mixture was cooled to room temperature, low boiling volatiles were removed under reduced pressure. The mixture was diluted with H₂O (3 L) and allowed to stand at room temperature overnight. The liquid layer was decanted, and the solid residue was dissolved in EtOAc (3 L) (required heating at 50 °C with stirring). The organic layer was washed with H₂O (130 mL), 0.5 N HCl (30 mL), and H₂O (50 mL) and dried (MgSO₄). The organic layer was concentrated to approximately 250 mL total volume and subjected to filtration to give the desired product (48.17 g) as a beige solid. The mother liquor was concentrated and subjected to recrystallization (EtOAc) to give a second portion of the desired product (5.27 g, 71% overall yield). ¹H NMR (400 MHz, CDCl₃) δ 2.73 (s, 3H), 2.93 (s, 3H), 3.01 (s, 3H), 4.23 and 4.48 (ABq, J_{AB} = 16.7 Hz, 2H), 4.62 and 4.70 (ABq, J_{AB} = 17.5 Hz, 2H), 5.04 and 5.09 (ABq, J_{AB} = 11.8 Hz, 2H), 7.00 (d, J = 8.3 Hz, 1H), 7.05–7.15 (m, 3H), 7.20–7.38 (m, 4H). ¹³C NMR (125 MHz, CDCl₃) δ 172.28, 167.17, 166.68, 165.77, 163.36, 160.21, 142.44, 135.28, 134.37, 133.76, 131.07, 130.24, 129.00, 128.89, 128.58, 128.46, 126.54, 120.95, 67.66, 52.05, 43.27, 36.38, 35.63, 23.66. HPLC (gradient from 100% A/0% B to 0% A/100% B (A = 90% H₂O/10% MeOH + 0.2% H₃PO₄) (B = 90% MeOH/10% H₂O + 0.2% H₃PO₄) for 8 min; detection at 220 nm. Zorbax SB C18 4.6 mm × 75 mm column): t_R = 7.97 min. m/z = 512 [M + H]⁺.

3-(Chloromethyl)-4-(2,4-dichlorophenyl)-2,7-dimethyl-6-phenyl-6,7-dihydropyrrolo[3,4-b]pyridin-5-one (10a). A mixture of **9a** (183 mg, 0.43 mmol) and lithium hydroxide (~200 mg) in THF/H₂O (4 mL) was allowed to stir at ambient temperature for 18 h. The mixture was then heated in a microwave reactor for 1 h at 120 °C. The reaction was quenched with 1 N HCl, and the aqueous portion was extracted into EtOAc. The combined organic layer was washed with brine, dried (Na₂SO₄), and evaporated to give the crude acid product (34 mg, 19% yield) as a pale yellow solid. ¹H NMR (400 MHz, CDCl₃) δ 2.80 (s, 3H), 4.85 and 4.95 (ABq, J = 17.6 Hz, 2H), 7.15 (t, J = 7.5 Hz, 1H), 7.20 (d, J = 7.9 Hz, 1H), 7.30 (dd, J = 8.9, 1.8 Hz, 1H), 7.37 (t, J = 7.9 Hz, 2H), 7.49 (d, J = 2.2 Hz, 1H), 7.76 (d, J = 7.9 Hz, 2H). m/z = 413 [M + H]⁺. To a solution of the acid (25 mg, 0.06 mmol) in THF was added ethyl chloroformate (24 μL, 0.25 mmol) followed by addition of triethylamine (50 μL, 0.36 mmol). Immediate precipitation was seen. The mixture was stirred at ambient temperature for 2 h, filtered, and washed with THF (1 mL × 2). NaBH₄ (11 mg, 0.29 mmol) in H₂O (0.3 mL) was added dropwise to the filtrate. The mixture was allowed to stir at ambient temperature for 18 h and then diluted with EtOAc/H₂O. The organic layer was washed with brine, dried (Na₂SO₄), and evaporated to give the alcohol (11.5 mg) as a colorless oil. To a solution of the alcohol (11.5 mg, 0.03 mmol) and triethylamine (30 μL, 0.22 mmol) in dichloromethane (2 mL) was added mesyl chloride (15 μL, 0.19 mmol). The mixture was allowed to stir at ambient temperature for 4 h. The solvent was evaporated, and the residue was purified by flash chromatography (4 g column, 0–100% EtOAc/hexanes) to give **10a** (4 mg, 33%) as a colorless oil. ¹H NMR (400 MHz, CDCl₃) δ 2.89 (s, 3H), 4.31 and 4.56 (ABq, J = 11.9 Hz, 2H), 4.87 and 4.93 (ABq, J = 17.6 Hz, 2H), 7.16 (t, J = 7.5 Hz, 1H), 7.29 (d, J = 8.4 Hz, 1H), 7.38 (t, J = 7.9 Hz, 2H), 7.42 (dd, J = 8.1, 2.0 Hz, 1H), 7.57 (d, J = 2.2 Hz, 1H), 7.78 (d, J = 7.9 Hz, 2H). m/z = 418 [M + H]⁺.

3-(Chloromethyl)-4-(2,4-dichlorophenyl)-6-(4-methoxyphenyl)-2-methyl-6,7-dihydropyrrolo[3,4-b]pyridin-5-one (10b). A mixture of **9b** (114.6 mg, 0.2 mmol) and 10% Pd/C (44 mg) in ethyl acetate (15 mL) was stirred under a H₂ (g) balloon at ambient temperature for 5 h. The reaction mixture was filtered and the filtrate evaporated to give the acid (114 mg, 0.3 mmol). The acid was dissolved in THF (10 mL), and ethyl chloroformate (50 μL, 0.5 mmol) and

triethylamine (150 μL, 1.1 mmol) were added sequentially. The mixture was stirred at ambient temperature for 2 h and then filtered. NaBH₄ (50 mg, 1.3 mmol) was added to the filtrate and the mixture stirred at ambient temperature for 18 h. The reaction was quenched with saturated aqueous NaHCO₃ and extracted into EtOAc. The combined organic layer was washed with brine, dried (Na₂SO₄), and evaporated. The residue was purified by flash chromatography (12 g column, EtOAc/hexanes) to give the alcohol (10.5 mg, 10% yield) as a white solid. m/z = 429 [M + H]⁺. To a solution of the alcohol (10 mg, 0.02 mmol) in dichloromethane (4 mL) were added triethylamine (25 μL, 0.18 mmol) and mesyl chloride (20 μL, 0.26 mmol). The mixture was allowed to stir at ambient temperature for 18 h and was evaporated. The residue was purified by flash chromatography (4 g column, EtOAc/hexanes) to give **10b** (7 mg, 67% yield) as a colorless oil. ¹H NMR (400 MHz, CDCl₃) δ 2.89 (s, 3H), 3.80 (s, 3H), 4.31 and 4.56 (ABq, J = 11.9 Hz, 2H), 4.82 and 4.89 (ABq, J = 17.1 Hz, 2H), 6.87–6.94 (m, 2H), 7.29 (d, J = 7.9 Hz, 1H), 7.41 (dd, J = 7.9, 1.8 Hz, 1H), 7.56 (d, J = 1.8 Hz, 1H), 7.63–7.70 (m, 2H). m/z = 447 [M + H]⁺.

2-(3-(Chloromethyl)-4-(2,4-dichlorophenyl)-2-methyl-5-oxo-5H-pyrrolo[3,4-b]pyridin-6(7H)-yl)-N,N-dimethylacetamide (10s). ¹H NMR (400 MHz, CDCl₃) δ 2.85 (s, 3H), 2.92 (s, 3H), 3.00 (s, 3H), 4.23 and 4.47 (ABq, J_{AB} = 16.3 Hz, 2H), 4.29 and 4.54 (ABq, J_{AB} = 11.9 Hz, 2H), 4.60 and 4.69 (ABq, J_{AB} = 17.5 Hz, 2H), 7.25 (d, J = 8.3 Hz, 1H), 7.37 (dd, J = 8.3, 2.2 Hz, 1H), 7.52 (d, J = 2.2 Hz, 1H). ¹³C NMR (125 MHz, CDCl₃) δ 67.22, 166.17, 162.90, 162.62, 143.95, 135.58, 133.60, 130.99, 130.75, 129.27, 127.09, 121.57, 51.95, 43.29, 39.83, 36.35, 35.63, 22.99. HPLC (gradient from 100% A/0% B to 0% A/100% B (A = 90% H₂O/10% MeOH + 0.2% H₃PO₄) (B = 90% MeOH/10% H₂O + 0.2% H₃PO₄) for 4 min; detection at 220 nm. YMC S5 ODS 4.6 mm × 50 mm, Ballistic column): t_R = 3.81 min. m/z = 427 [M + H]⁺.

3-(Aminomethyl)-4-(2,4-dichlorophenyl)-6-(4-methoxyphenyl)-2-methyl-6,7-dihydropyrrolo[3,4-b]pyridin-5-one, TFA Salt (1b). A mixture of **10b** (7 mg, 0.02 mmol) and 7 M NH₃ in MeOH (4 mL) was heated in a microwave reactor at 100 °C for 15 min. The solvent was removed in vacuo, and the residue was purified by preparative HPLC (Phenomenex, 10 min gradient, 30–100% B) to give **1b** (6.7 mg, 79% yield) as a TFA salt. ¹H NMR (400 MHz, CDCl₃) δ 2.86 (s, 3H), 3.80 (s, 3H), 3.97 and 4.20 (ABq, J = 14.5 Hz, 2H), 4.96 and 5.01 (ABq, J = 18.0 Hz, 2H), 6.94–7.00 (m, 2H), 7.36 (d, J = 8.4 Hz, 1H), 7.54 (dd, J = 8.4, 2.2 Hz, 1H), 7.59–7.65 (m, 2H), 7.72 (d, J = 1.8 Hz, 1H). HRMS calculated for C₂₂H₂₀Cl₂N₃O₂: 428.0933. Found: 428.0943. Analytical HPLC method: t_R = 6.1 min.

3-(Aminomethyl)-4-(2,4-dichlorophenyl)-2-methyl-6-phenyl-6,7-dihydropyrrolo[3,4-b]pyridin-5-one, TFA Salt (1a). ¹H NMR (400 MHz, CDCl₃ + CD₃OD as cosolvent) δ 2.83 (s, 3H), 3.88 and 4.10 (ABq, J = 14.5 Hz, 2H), 4.85 and 4.90 (ABq, J = 18.5 Hz, 2H), 7.14 (t, J = 7.0 Hz, 1H), 7.24–7.27 (m, 1H), 7.34 (t, J = 7.9 Hz, 2H), 7.40 (dd, J = 8.1, 2.0 Hz, 1H), 7.55 (d, J = 1.8 Hz, 1H), 7.70 (d, J = 8.8 Hz, 2H). HRMS calculated for C₂₁H₁₈Cl₂N₃O: 398.0827. Found: 398.0812.

3-(Aminomethyl)-4-(2,4-dichlorophenyl)-6-(2-methoxyphenyl)-2-methyl-6,7-dihydropyrrolo[3,4-b]pyridin-5-one, TFA Salt (1c). ¹H NMR (400 MHz, CDCl₃) δ 2.87 (s, 3H), 3.83 (s, 3H), 3.99 and 4.22 (ABq, J = 14.5 Hz, 2H), 4.85–4.95 (m, 2H), 7.01 (broad t, J = 7.5 Hz, 1H), 7.14 (broad d, J = 8.4 Hz, 1H), 7.32 (dd, J = 7.9, 1.8 Hz, 1H), 7.34–7.40 (m, 2H), 7.52 (dd, J = 8.4, 2.2 Hz, 1H), 7.69 (d, J = 2.2 Hz, 1H). HRMS calculated for C₂₂H₂₀Cl₂N₃O₂: 428.0933. Found: 428.0937.

3-(Aminomethyl)-4-((S)-2,4-dichlorophenyl)-6-(2-methoxyphenyl)-2-methyl-6,7-dihydropyrrolo[3,4-b]pyridin-5-one, TFA Salt (2a) and 3-(Aminomethyl)-4-((R)-2,4-dichlorophenyl)-6-(2-methoxyphenyl)-2-methyl-6,7-dihydropyrrolo[3,4-b]pyridin-5-one, TFA Salt (3a). **1c** was separated on a Chiralcel OJ, 20 μm, 5 cm × 50 cm column using an isocratic gradient of 15% EtOH–MeOH (50%) in heptane to afford individual enantiomers **2a** and **3a**. **2a** (faster-eluting): [α]_D²⁵ +8.2°. Purity by chiral analytical HPLC [Chiralcel OJ 4.6 mm × 250 mm; 15% EtOH–MeOH (1:1; containing 0.1% DEA) in heptane (containing 0.1% DEA)]: >98%. **3a** (slower-eluting): [α]_D²⁵ –8.0°. Purity by chiral analytical HPLC [Chiralcel OJ 4.6 mm × 250 mm; 15% EtOH–MeOH (1:1; containing 0.1% DEA) in heptane (containing 0.1% DEA)]: >98%. The more potent atropisomer, **3a**, was assigned the

Sa stereochemistry based on analogy to a cocrystal structure of a close analogue (compound (+)-3f in ref 6c). Analytical HPLC: $t_R = 4.8$ min.

3-(Aminomethyl)-4-(2,4-dichlorophenyl)-6-(2-methoxyethyl)-2-methyl-6,7-dihydropyrrolo[3,4-b]pyridin-5-one, TFA Salt (1e, BMS-744891). $^1\text{H NMR}$ (400 MHz, CDCl_3) δ 2.83 (s, 3H), 3.34 (s, 3H), 3.58–3.63 (m, 2H), 3.65–3.78 (m, 2H), 3.95 and 4.18 (AB_q, $J = 14.5$ Hz, 2H), 4.62 (s, 2H), 7.33 (d, $J = 8.4$ Hz, 1H), 7.52 (dd, $J = 8.1$, 2.0 Hz, 1H), 7.70 (d, $J = 2.2$ Hz, 1H). HRMS calculated for $\text{C}_{18}\text{H}_{20}\text{Cl}_2\text{N}_3\text{O}_2$: 380.0933. Found: 380.0941. An X-ray cocrystal structure of **1e**/DPP4 was obtained.^{12c} It is presumed that the more active atropisomer (**2f**) crystallized with the protein under the crystallization conditions.

3-(Aminomethyl)-4-(2,4-dichlorophenyl)-2-methyl-6,7-dihydropyrrolo[3,4-b]pyridin-5-one, TFA Salt (1f). $^1\text{H NMR}$ (400 MHz, CDCl_3) δ 2.84 (s, 3H), 3.95 and 4.19 (AB_q, $J = 14.9$ Hz, 2H), 4.49 (s, 2H), 7.33 (d, $J = 8.4$ Hz, 1H), 7.48–7.55 (m, 1H), 7.66–7.72 (m, 1H). HRMS calculated for $\text{C}_{15}\text{H}_{14}\text{Cl}_2\text{N}_3\text{O}$: 322.0514. Found: 322.0512.

Ethyl 3-(Aminomethyl)-4-(2,4-dichlorophenyl)-2-methyl-5-oxo-5H-pyrrolo[3,4-b]pyridine-6(7H)-carboxylate, TFA Salt (1g). A mixture of **1f** (47 mg, 0.096 mmol), 1 M Boc_2O /THF (0.18 mL, 0.18 mmol), NaHCO_3 (160 mg, 1.9 mmol), and THF (5 mL) was stirred at room temperature overnight. The mixture was taken up in EtOAc and H_2O and transferred to a separatory funnel. The aqueous layer was extracted with EtOAc ($\times 2$), washed with brine, dried over Na_2SO_4 , filtered, and evaporated to yield the crude product which was used as such for the next step without purification. $m/z = 422$ [$\text{M} + \text{H}$]⁺. To a solution of the above crude product in CH_2Cl_2 (5 mL) was added Et_3N (0.1 mL, 0.72 mmol) followed by EtOCOCl (0.04 mL, 0.42 mmol), and the mixture was stirred at room temperature overnight. LC indicated $\sim 10\%$ conversion. DMAP (10 mg) followed by additional EtOCOCl (0.1 mL, 1.05 mmol) was added and mixture allowed to stir at room temperature overnight. Evaporation and flash chromatography (40 g silica, 0–100% EtOAc/hexanes) yielded the carbamate (18.5 mg, 39% two steps) as a colorless oil. $m/z = 494$ [$\text{M} + \text{H}$]⁺. To a solution of the carbamate (18 mg, 0.046 mmol) in CH_2Cl_2 (1 mL) was added TFA (1 mL) dropwise and the mixture stirred at room temperature for 1 h. Mixture was evaporated and purified by PrepHPLC (Phenomenex LUNA 5 μm C18(2) 21.2 mm \times 100 mm; 8 min gradient; 0–100% B; 20 mL/min) to yield **1g** (16.8 mg, 91%) as a white powder. Analytical HPLC: $t_R = 5.2$ min.

3-(Aminomethyl)-4-((S)-2,4-dichlorophenyl)-6-((S)-1-methoxypropan-2-yl)-2-methyl-6,7-dihydropyrrolo[3,4-b]pyridin-5-one, TFA Salt (2g). $^1\text{H NMR}$ (400 MHz, CD_3OD) δ 1.26 (d, $J = 7.0$ Hz, 3H), 2.83 (s, 3H), 3.32 (s, 3H), 3.49 (dd, $J = 10.1$, 4.4 Hz, 1H), 3.59 (dd, $J = 12.1$, 7.9 Hz, 1H), 3.95 and 4.18 (AB_q, $J = 14.5$ Hz, 2H), 4.52–4.54 (m, 1H), 4.50 and 4.55 (AB_q, $J = 18.9$ Hz, 2H), 7.32 (d, $J = 8.4$ Hz, 1H), 7.52 (dd, $J = 8.4$, 1.8 Hz, 1H), 7.70 (d, $J = 2.2$ Hz, 1H). HRMS calculated for $\text{C}_{19}\text{H}_{22}\text{Cl}_2\text{N}_3\text{O}_2$: 394.1089. Found: 394.1104 [$\text{M} + \text{H}$]⁺.

3-(Aminomethyl)-4-((R)-2,4-dichlorophenyl)-6-((S)-1-methoxypropan-2-yl)-2-methyl-6,7-dihydropyrrolo[3,4-b]pyridin-5-one, TFA Salt (3b). $^1\text{H NMR}$ (400 MHz, CD_3OD) δ 1.27 (d, $J = 7.0$ Hz, 3H), 2.83 (s, 3H), 3.31 (s, 3H), 3.49 (dd, $J = 10.1$, 4.4 Hz, 1H), 3.59 (dd, $J = 10.1$, 7.9 Hz, 1H), 3.94 and 4.18 (AB_q, $J = 14.5$ Hz, 2H), 4.46–4.55 (m, 1H), 4.48 and 4.57 (AB_q, $J = 18.5$ Hz, 2H), 7.33 (d, $J = 8.4$ Hz, 1H), 7.52 (dd, $J = 8.4$, 2.2 Hz, 1H), 7.70 (d, $J = 2.2$ Hz, 1H). LCMS: 394.10 [$\text{M} + \text{H}$]⁺. HRMS calculated for $\text{C}_{19}\text{H}_{22}\text{Cl}_2\text{N}_3\text{O}_2$: 394.1089. Found: 394.1073 [$\text{M} + \text{H}$]⁺.

(R)-2-(3-(Aminomethyl)-4-(2,4-dichlorophenyl)-2-methyl-5-oxo-5H-pyrrolo[3,4-b]pyridin-6(7H)-yl)-N,N-dimethylacetamide, TFA Salt (3e). The pure enantiomer was obtained by supercritical fluid chromatography (chiralpak AD-H 250 mm \times 30 mm i.d.; 5 μm ; flow rate, 120 mL/min; mobile phase, CO_2 /EtOH 75/25 (with 0.1%DEA)). This product was further purified by prep HPLC (Phenomenex Luna 5 μm C18, 21.2 mm \times 100 mm; 10 min gradient from 85% A/15% B to 0% A/100% B (A = 90% H_2O /10% MeOH + 0.1% TFA) (B = 90% MeOH/10% H_2O + 0.1% TFA); detection at 220 nm) to give **3e** as white solid. $^1\text{H NMR}$ (400 MHz, CD_3OD) δ 2.83 (s, 3H), 2.94 (s, 3H), 3.07 (s, 3H), 3.95 and 4.19 (AB_q, $J = 18.0$ Hz, 2H), 4.38 and 4.53 (AB_q, $J = 18.0$ Hz, 2H), 4.58 (s, 2H), 7.33 (d, $J = 8.3$ Hz, 1H), 7.52 (dd, $J = 8.3$, 2.2 Hz, 1H), 7.69 (d, $J = 2.2$ Hz, 1H). HRMS: calculated for $\text{C}_{19}\text{H}_{20}\text{Cl}_2\text{N}_4\text{O}_2$: 406.0963. Found: 407.1032 [$\text{M} + \text{H}$]⁺.

(S)-3-(Aminomethyl)-4-(2,4-dichlorophenyl)-2-methyl-6-(1-methyl-1H-pyrazol-3-yl)-6,7-dihydro-5H-pyrrolo[3,4-b]pyridin-5-one, TFA Salt (2b). $^1\text{H NMR}$ (400 MHz, CD_3OD) δ 2.86 (s, 3H), 3.86 (s, 3H), 3.97 and 4.20 (AB_q, $J = 14.5$ Hz, 2H), 4.98 (br s, 2H), 6.65 (d, $J = 2.2$ Hz, 1H), 7.36 (d, $J = 8.4$ Hz, 1H), 7.52 (d, $J = 2.6$ Hz, 1H), 7.55 (dd, $J = 8.4$, 2.2 Hz, 1H), 7.73 (d, $J = 1.8$ Hz, 1H). HRMS calculated for $\text{C}_{19}\text{H}_{18}\text{Cl}_2\text{N}_5\text{O}$: 402.0888. Found: 402.0891 [$\text{M} + \text{H}$]⁺.

(S)-3-(Aminomethyl)-4-(2,4-dichlorophenyl)-2-methyl-6-((1-methyl-1H-pyrazol-3-yl)methyl)-6,7-dihydro-5H-pyrrolo[3,4-b]pyridin-5-one, TFA Salt (2c). $^1\text{H NMR}$ (400 MHz, CD_3OD) δ 2.82 (s, 3H), 3.34 (s, 2H), 3.85 (s, 3H), 3.95 and 4.19 (AB_q, $J = 14.1$ Hz, 2H), 4.66 and 4.72 (AB_q, $J = 15.2$ Hz, 2H), 6.18 (d, $J = 2.2$ Hz, 1H), 7.35 (d, $J = 8.4$ Hz, 1H), 7.48–7.57 (m, 1H), 7.70 (d, $J = 2.2$ Hz, 1H). HRMS calculated for $\text{C}_{20}\text{H}_{20}\text{Cl}_2\text{N}_5\text{O}_2$: 416.1045. Found: 416.1046 [$\text{M} + \text{H}$]⁺.

(S)-3-(Aminomethyl)-4-(2,4-dichlorophenyl)-2-methyl-6-(oxazol-2-ylmethyl)-6,7-dihydro-5H-pyrrolo[3,4-b]pyridin-5-one, TFA Salt (2d). $^1\text{H NMR}$ (500 MHz, CD_3OD) δ 2.74 (s, 3H), 3.86 and 4.10 (AB_q, $J = 14.3$ Hz, 2H), 4.53 and 4.57 (AB_q, $J = 19.0$ Hz, 2H), 4.75 and 4.83 (AB_q, $J = 16.5$ Hz, 2H), 7.03 (s, 1H), 7.25 (d, $J = 8.3$ Hz, 1H), 7.41 (dd, $J = 8.3$, 2.20 Hz, 1H), 7.59 (d, $J = 1.7$ Hz, 1H), 7.79 (s, 1H). HRMS calculated for $\text{C}_{19}\text{H}_{17}\text{Cl}_2\text{N}_4\text{O}_2$: 403.0729. Found: 403.0715 [$\text{M} + \text{H}$]⁺.

(S)-3-(Aminomethyl)-4-(2,4-dichlorophenyl)-2-methyl-6-((5-methylisoxazol-3-yl)methyl)-6,7-dihydro-5H-pyrrolo[3,4-b]pyridin-5-one, TFA Salt (2e). $^1\text{H NMR}$ (400 MHz, CD_3OD) δ 2.38 (s, 3H), 2.82 (s, 3H), 3.94 and 4.18 (AB_q, $J = 14.5$ Hz, 2H), 4.57 (s, 2H), 4.72 and 4.78 (AB_q, $J = 15.8$ Hz, 2H), 6.08 (s, 1H), 7.32 (d, $J = 8.3$ Hz, 1H), 7.53 (dd, $J = 8.3$, 2.0 Hz, 1H), 7.71 (d, $J = 2.0$ Hz, 1H). HRMS, Anal. Calcd for $\text{C}_{20}\text{H}_{19}\text{Cl}_2\text{N}_4\text{O}_2$: 417.0885. Found: 417.0869 [$\text{M} + \text{H}$]⁺.

(S)-3-(Aminomethyl)-4-(2,4-dichlorophenyl)-6-(2-methoxyethyl)-2-methyl-6,7-dihydro-5H-pyrrolo[3,4-b]pyridin-5-one, TFA Salt (2f). $^1\text{H NMR}$ (400 MHz, CD_3OD) δ 2.83 (s, 3H), 3.34 (s, 3H), 3.60 (t, $J = 5.3$ Hz, 2H), 3.65–3.80 (m, 2H), 4.18 (AB_q, $J = 14.5$ Hz, 2H), 4.62 (s, 2H), 7.33 (d, $J = 8.4$ Hz, 1H), 7.52 (dd, $J = 8.1$, 2.0 Hz, 1H), 7.69 (d, $J = 2.2$ Hz, 1H). HRMS calculated for $\text{C}_{18}\text{H}_{20}\text{Cl}_2\text{N}_3\text{O}_2$: 380.0933. Found: 380.0929 [$\text{M} + \text{H}$]⁺. Stereochemistry assigned by X-ray cocrystal structure of **1e** with DPP4.^{12c} It is presumed that the more active atropisomer (**2f**) cocrystallized with the protein under the crystallization conditions.

(S)-3-(Aminomethyl)-4-(2,4-dichlorophenyl)-2-methyl-6-(((R)-tetrahydrofuran-2-yl)methyl)-6,7-dihydro-5H-pyrrolo[3,4-b]pyridin-5-one, TFA Salt (2h). $^1\text{H NMR}$ (400 MHz, CD_3OD) δ 1.53–1.65 (m, 1H), 1.83–1.94 (m, 2H), 1.95–2.06 (m, 1H), 2.83 (s, 3H), 3.52 (dd, $J = 14.1$, 7.9 Hz, 1H), 3.66–3.76 (m, 2H), 3.82–3.90 (m, 1H), 3.95 and 4.18 (AB_q, $J = 14.5$ Hz, 2H), 4.06–4.15 (m, 1H), 4.60 and 4.71 (AB_q, $J = 18.9$ Hz, 2H), 7.33 (d, $J = 7.91$ Hz, 1H), 7.52 (dd, $J = 8.1$, 2.0 Hz, 1H), 7.69 (d, $J = 1.8$ Hz, 1H). HRMS calculated for $\text{C}_{20}\text{H}_{22}\text{Cl}_2\text{N}_3\text{O}_2$: 406.1089. Found: 406.1085 [$\text{M} + \text{H}$]⁺. [α]_D²⁵ –15.08° (c 1.9, EtOH).

(S)-3-(Aminomethyl)-4-(2,4-dichlorophenyl)-2-methyl-6-(((S)-tetrahydrofuran-2-yl)methyl)-6,7-dihydro-5H-pyrrolo[3,4-b]pyridin-5-one, TFA Salt (2i). $^1\text{H NMR}$ (400 MHz, CD_3OD) δ 1.53–1.65 (m, 1H), 1.83–1.94 (m, 2H), 1.95–2.06 (m, 1H), 2.83 (s, 3H), 3.49 (dd, $J = 14.5$, 7.7 Hz, 1H), 3.66–3.76 (m, 2H), 3.82–3.90 (m, 1H), 3.95 and 4.19 (AB_q, $J = 14.5$ Hz, 2H), 4.06–4.15 (m, 1H), 4.63 and 4.71 (AB_q, $J = 18.9$ Hz, 2H), 7.34 (d, $J = 7.91$ Hz, 1H), 7.51 (dd, $J = 8.4$, 1.8 Hz, 1H), 7.68 (d, $J = 2.2$ Hz, 1H). HRMS calculated for $\text{C}_{20}\text{H}_{22}\text{Cl}_2\text{N}_3\text{O}_2$: 406.1089. Found: 406.1092 [$\text{M} + \text{H}$]⁺. [α]_D²⁵ +10.27° (c 2.2, EtOH).

(S)-3-(Aminomethyl)-4-(2,4-dichlorophenyl)-2-methyl-6-(((S)-pyrrolidin-2-ylmethyl)-6,7-dihydro-5H-pyrrolo[3,4-b]pyridin-5-one, TFA Salt (2j). A mixture of **11c** (28 mg, 0.055 mmol) and TFA (0.7 mL) in CH_2Cl_2 (1.0) was allowed to stir at ambient temperature for 1 h and evaporated under reduced pressure. The residue was purified by preparative HPLC (Luna 5 μm C18 (2), 30 mm \times 100 mm, 10 min gradient, 0–60% solvent B, 40 mL/min) to give **2j** (15.9 mg, 45.7% yield) as an off-white solid. $^1\text{H NMR}$ (400 MHz, CD_3OD) δ 1.59–1.75 (m, 1H), 1.83–2.05 (m, 2H), 2.07–2.18 (m, 1H), 2.75 (s, 3H), 3.10–3.30 (m, 2H), 3.64–3.98 (m, 4H), 4.12 (part of AB_q, $J = 14.1$ Hz, 1H), 4.50 and 4.61 (AB_q, $J = 18.0$ Hz, 2H), 7.26 (d, $J = 8.4$ Hz, 1H), 7.42 (dd, $J = 8.1$, 2.0 Hz, 1H), 7.60 (d, $J = 2.20$ Hz, 1H). HRMS calculated

for $C_{20}H_{23}Cl_2N_4O$: 405.1249. Found: 405.1256 $[M + H]^+$. Analytical HPLC: $t_R = 1.4$ min.

(S)-3-(3-(Aminomethyl)-4-(2,4-dichlorophenyl)-2-methyl-5-oxo-5H-pyrrolo[3,4-b]pyridin-6(7H)-yl)propanoic Acid, TFA Salt (2m). 1H NMR (400 MHz, CD_3OD) δ 2.67 (t, $J = 6.8$ Hz, 2H), 2.83 (s, 3H), 3.73–3.85 (m, 2H), 3.94 and 4.18 (AB_q , $J = 14.5$ Hz, 2H), 4.62 (s, 2H), 7.32 (d, $J = 8.4$ Hz, 1H), 7.52 (dd, $J = 8.1, 2.0$ Hz, 1H), 7.70 (d, $J = 1.8$ Hz, 1H). HRMS calculated for $C_{18}H_{18}Cl_2N_3O_3$: 394.0725. Found: 394.0735 $[M + H]^+$.

(S)-3-(3-(Aminomethyl)-4-(2,4-dichlorophenyl)-2-methyl-5-oxo-5H-pyrrolo[3,4-b]pyridin-6(7H)-yl)-N,N-diethylpropanamide, TFA Salt (2o). 1H NMR (400 MHz, CD_3OD) δ 1.06 (t, $J = 7.0$ Hz, 3H), 1.14 (t, $J = 7.0$ Hz, 3H), 2.54–2.80 (m, 2H), 2.83 (s, 3H), 3.32–3.38 (m, 4H), 3.82 (t, $J = 6.8$ Hz, 2H), 3.94 and 4.18 (AB_q , $J = 14.5$ Hz, 2H), 4.60 and 4.65 (AB_q , $J = 18.9$ Hz, 2H), 7.32 (d, $J = 8.40$ Hz, 1H), 7.51 (dd, $J = 8.1, 2.0$ Hz, 1H), 7.69 (d, $J = 1.8$ Hz, 1H). HRMS calculated for $C_{22}H_{27}Cl_2N_4O_2$: 449.1511. Found: 449.1506 $[M + H]^+$.

(R)-2-((S)-3-(Aminomethyl)-4-(2,4-dichlorophenyl)-2-methyl-5-oxo-5H-pyrrolo[3,4-b]pyridin-6(7H)-yl)-N,N-diethylpropanamide, TFA Salt (2p). 1H NMR (400 MHz, CD_3OD) possible rotamers; data for major rotamer: δ 1.09 (t, $J = 7.3$ Hz, 3H), 1.20 (t, $J = 7.0$ Hz, 3H), 1.52 (d, $J = 7.0$ Hz, 3H), 2.84 (s, 3H), 3.18–3.28 (m, 4H), 3.93 and 4.20 (AB_q , $J = 14.5$ Hz, 2H), 4.67 and 4.80 (AB_q , $J = 18.0$ Hz, 2H), 5.24 (q, $J = 7.0$ Hz, 1H), 7.33 (d, $J = 8.4$ Hz, 1H), 7.52 (dd, $J = 8.4, 2.2$ Hz, 1H), 7.69 (d, $J = 2.2$ Hz, 1H). HRMS calculated for $C_{22}H_{27}Cl_2N_4O_2$: 449.1511. Found: 449.1524 $[M + H]^+$.

(S)-3-(Aminomethyl)-6-(((S)-1-(cyclopropylsulfonyl)pyrrolidin-2-yl)methyl)-4-(2,4-dichlorophenyl)-2-methyl-6,7-dihydro-5H-pyrrolo[3,4-b]pyridin-5-one, TFA Salt (2k). 1H NMR (500 MHz, CD_3OD) δ 0.81–0.97 (m, 4H), 1.65–1.74 (m, 1H), 1.81–1.93 (m, 2H), 1.91–2.03 (m, 1H), 2.33–2.50 (m, 1H), 2.73 (s, 3H), 3.24–3.31 (m, 1H), 3.34–3.61 (m, 3H), 3.85 (part of AB_q , $J = 14.3$ Hz, 1H), 4.06–4.18 (m, 2H), 4.50–4.66 (m, 2H), 7.24 (d, $J = 8.3$ Hz, 1H), 7.42 (d, $J = 8.3$ Hz, 1H), 7.59 (s, 1H). HRMS calculated for $C_{23}H_{27}Cl_2N_4O_3S$: 509.1181. Found: 509.1190 $[M + H]^+$.

(R)-3-(Aminomethyl)-4-(2,4-dichlorophenyl)-6-(2-methoxyethyl)-2-methyl-6,7-dihydro-5H-pyrrolo[3,4-b]pyridin-5-one, TFA Salt (3c). 1H NMR (400 MHz, CD_3OD) δ 2.83 (s, 3H), 3.34 (s, 3H), 3.60 (t, $J = 5.1$ Hz, 2H), 3.65–3.80 (m, 2H), 3.95 and 4.19 (AB_q , $J = 14.5$ Hz, 2H), 4.62 (s, 2H), 7.33 (d, $J = 8.4$ Hz, 1H), 7.52 (dd, $J = 8.4, 2.2$ Hz, 1H), 7.69 (d, $J = 1.8$ Hz, 1H). HRMS calculated for $C_{18}H_{20}Cl_2N_3O_2$: 380.0933. Found: 380.0931 $[M + H]^+$.

Benzyl 6-(2-tert-Butoxy-2-oxoethyl)-4-(2,4-dichlorophenyl)-2-methyl-5-oxo-6,7-dihydro-5H-pyrrolo[3,4-b]pyridine-3-carboxylate (9h). A mixture of **8b** (10.59 g, 21.43 mmol), glycine *tert*-butyl ester hydrochloride (8.26 g, 49.29 mmol), and triethylamine (8.94 mL, 64.29 mmol) in *N,N*-dimethylacetamide (200 mL) was heated to 100 °C for 2 h and then cooled to ambient temperature. The resulting mixture was partitioned between EtOAc and H_2O , and the aqueous layer was extracted further with EtOAc (2 \times). The combined organic extracts were washed with H_2O and brine, dried (Na_2SO_4), and evaporated under reduced pressure. The residue was purified by flash chromatography (330 g column, 0–100% EtOAc/hexanes) to give **9h** (9.34 g, 77% yield) as a light yellow solid. 1H NMR (500 MHz, $CDCl_3$) δ 1.44 (s, 9H), 2.74 (s, 3H), 4.13 and 4.29 (AB_q , $J = 17.6$ Hz, 2H), 4.56 (s, 2H), 5.05 and 5.07 (AB_q , $J = 11.8, 2$ Hz), 7.00 (d, $J = 8.3$ Hz, 1H), 7.06–7.16 (m, 2H), 7.21–7.40 (m, 5H). $m/z = 541$ $[M + H]^+$.

6-(2-tert-Butoxy-2-oxoethyl)-4-(2,4-dichlorophenyl)-2-methyl-5-oxo-6,7-dihydro-5H-pyrrolo[3,4-b]pyridine-3-carboxylic Acid (15). A mixture of **9h** (9.33 g, 17.23 mmol) and 10% palladium on carbon (1.36 g) in EtOAc (150 mL) was stirred in the presence of hydrogen (balloon) at ambient temperature for 2 h. The reaction mixture was filtered through a pad of Celite and washed with MeOH and CH_2Cl_2 . The filtrate was evaporated under reduced pressure to give crude **15** (8.13 g, 100% yield) as a dark yellow solid. 1H NMR (400 MHz, CD_3OD) δ 1.45 (s, 9H), 2.75 (s, 3H), 4.23 and 4.28 (AB_q , $J = 18.0$ Hz, 2H), 4.63 and 4.58 (AB_q , $J = 18.0$ Hz, 2H), 7.27 (d, $J = 8.4$ Hz, 1H), 7.39 (dd, $J = 8.1, 2.0$ Hz, 1H), 7.55 (d, $J = 2.2$ Hz, 1H). $m/z = 451$ $[M + H]^+$.

tert-Butyl 2-(4-(2,4-Dichlorophenyl)-3-(hydroxymethyl)-2-methyl-5-oxo-5H-pyrrolo[3,4-b]pyridin-6(7H)-yl)acetate (16). To a stirred mixture of **15** (1.18 g, 2.5 mmol) and triphenylphosphine

resin (5.07 g, 7.5 mmol) in CH_2Cl_2 (80 mL) at ambient temperature was added trichloroacetonitrile (0.75 mL, 7.5 mmol) dropwise. The mixture was stirred at ambient temperature for 2.5 h, and additional triphenylphosphine resin (0.33 g, 0.5 mmol) and trichloroacetonitrile (50 μ L, 0.5 mmol) were added. After 30 min, the mixture was filtered and the filtrate was concentrated in vacuo to give an acid chloride (1.12 g) as a light yellow solid. To a solution of the above acid chloride (0.93 g, 1.98 mmol) in THF (30 mL) at 0 °C was added lithium *tert*-butoxyaluminumhydride dropwise during a period of 5 min. The mixture was stirred at 0 °C for 20 min, quenched with H_2O (1.3 mL), and concentrated in vacuo. Purification of the residue by flash chromatography (40 g column, 0–100% EtOAc/hexanes) afforded **16** (690.4 mg, 80% for 2 steps) as an off-white solid. 1H NMR (500 MHz, CD_3OD) δ 1.45 (s, 9H), 2.84 (s, 3H), 4.20 and 4.26 (AB_q , $J = 17.6, 2$ Hz), 4.32 and 4.58 (AB_q , $J = 12.1$ Hz, 2H), 4.56 (s, 2H), 7.32 (d, $J = 8.3$ Hz, 1H), 7.44 (d, $J = 8.3$ Hz, 1H), 7.59 (s, 1H). $m/z = 437$ $[M + H]^+$.

(R)-tert-Butyl 2-(3-(Chloromethyl)-4-(2,4-dichlorophenyl)-2-methyl-5-oxo-5H-pyrrolo[3,4-b]pyridin-6(7H)-yl)acetate (17). **16** (5.7 g) was separated by supercritical fluid chromatography (Chiralpak AD 250 mm \times 4.6 mm i.d.; 10 μ m; 35 °C; flow rate, 2.0 mL/min; mobile phase, CO_2 /IPA 82/18; injection volume, 5 μ L; detector wavelength, 220 nm) to give isomer A (2.43 g, $t_R = 5.1$ min, 100% ee) and isomer B (2.55 g, $t_R = 7.1$ min, 100% ee) as an off-white solid. To a mixture of isomer B (763 mg, 1.74 mmol) and Et_3N (0.97 mL, 6.98 mmol) in CH_2Cl_2 (15 mL) at 0 °C was added mesyl chloride (0.41 mL, 5.24 mmol) dropwise. The stirred mixture was kept at ambient temperature overnight and evaporated under reduced pressure. The residue was partitioned between EtOAc and H_2O , and the aqueous layer was extracted further with EtOAc (2 \times). The combined organic extracts were washed with brine, dried (Na_2SO_4), and concentrated in vacuo. The crude product was chromatographed (40 g column, 0–100% EtOAc/hexanes) to give **17** (785.7 mg, 99%) as a white solid. 1H NMR (500 MHz, $CDCl_3$) δ 1.45 (s, 9H), 2.86 (s, 3H), 4.14 and 4.29 (AB_q , $J = 17.6, 2$ Hz), 4.31 (part of AB_q , $J = 7.1, 1$ Hz), 4.52–4.60 (m, 3H), 7.27 (d, $J = 8.3, 1$ Hz), 7.39 (dd, $J = 8.3, 2.2$ Hz, 1H), 7.54 (d, $J = 1.7, 1$ Hz). $m/z = 455$ $[M + H]^+$.

(S)-2-(3-((tert-Butoxycarbonylamino)methyl)-4-(2,4-dichlorophenyl)-2-methyl-5-oxo-5H-pyrrolo[3,4-b]pyridin-6(7H)-yl)acetic Acid (18). A solution of **17** (784 mg, 1.72 mmol) in 7 M NH_3 in MeOH (140 mL) was heated at 50 °C for 50 min, cooled, and concentrated to give crude (*S*)-*tert*-butyl 2-(3-(aminomethyl)-4-(2,4-dichlorophenyl)-2-methyl-5-oxo-5H-pyrrolo[3,4-b]pyridin-6(7H)-yl)acetate (1.81 g) as a light orange sticky solid. To the above material in CH_2Cl_2 (8.0 mL) was added TFA (5.0 mL), and the resulting mixture was allowed to stir at ambient temperature for 3 h and evaporated under reduced pressure. The residue was coevaporated with ethanol several times to give crude (*S*)-2-(3-(aminomethyl)-4-(2,4-dichlorophenyl)-2-methyl-5-oxo-5H-pyrrolo[3,4-b]pyridin-6(7H)-yl)acetic acid as a yellow solid. The yellow solid was dissolved in THF (35 mL) and treated with saturated aqueous $NaHCO_3$ (20 mL) followed by di-*tert*-butyl dicarbonate (1.28 g, 5.85 mmol). The mixture was stirred at ambient temperature for 2.5 h, and then the pH of the mixture was adjusted to 3 with 1 N HCl. The aqueous layer was extracted with EtOAc (2 \times), and the combined organic extracts were washed with brine, dried (Na_2SO_4), and evaporated under reduced pressure to give crude **18** (1.375 g) as a light yellow solid which was used for the next step without further purification. $m/z = 480$ $[M + H]^+$.

2-(3-((Bis-tert-butoxycarbonylamino)methyl)-4-(2,4-dichlorophenyl)-2-methyl-5-oxo-5H-pyrrolo[3,4-b]pyridin-6(7H)-yl)-N,N-dimethylacetamide (19). To a stirred solution of **18** (8.28 g, 19.4 mmol) in THF (125 mL) at 60 °C was added di-*tert*-butyl iminodicyclohexylcarboxylate, potassium salt (9.95 g, 9.40 mmol). DMF (41.5 mL) was added and the reaction mixture heated at 60 °C for 5 min and stirred at room temperature for another 25 min. The reaction mixture was concentrated under reduced pressure to remove THF. The resulting residue was diluted with EtOAc (570 mL) and extracted with 5% LiCl solution (2 \times 380 mL) and brine. The aqueous layers were extracted with EtOAc (1 \times 400 mL, 1 \times 200 mL). The combined organic layers were dried ($MgSO_4$), filtered, and concentrated to give a yellow foam which was purified by silica gel chromatography (EtOAc) to give the desired product (7.19 g, 60%) as a white solid. 1H NMR (400 MHz,

CDCl_3) δ 1.36 (s, 18H), 2.81 (s, 3H), 2.93 (s, 3H), 3.00 (s, 3H), 4.22 and 4.46 (AB_q, J_{AB} = 16.5 Hz, 2H), 4.56 and 4.69 (AB_q, J_{AB} = 17.3 Hz, 2H), 4.66 and 4.91 (AB_q, J_{AB} = 15.2 Hz, 2H), 7.23 (d, J = 8.3 Hz, 1H), 7.30 (dd, J = 8.3, 2.2 Hz, 1H), 7.45 (d, J = 2.2 Hz, 1H). Analytical HPLC: t_R = 8.60 min. m/z = 607 [M + H]⁺.

(S)-2-(3-((Bis-*tert*-butoxycarbonylamino)methyl)-4-(2,4-dichlorophenyl)-2-methyl-5-oxo-5H-pyrrolo[3,4-*b*]pyridin-6(7H)-yl)-*N,N*-dimethylacetamide (20). The desired atropisomer (slower-eluting) was obtained by chiral SFC separation (Chiralpak AD 250 mm × 4.6 mm i.d.; 10 μ m; 35 °C; flow rate, 2.0 mL/min; mobile phase, CO₂/IPA 82/18; injection volume, 5 μ L; detector wavelength, 220 nm) in 96% recovery and >99% ee.

(S)-2-(3-(Aminomethyl)-4-(2,4-dichlorophenyl)-2-methyl-5-oxo-5H-pyrrolo[3,4-*b*]pyridin-6(7H)-yl)acetamide, TFA Salt (2q). To a mixture of 18 (70 mg, 0.146 mmol), HOBT·H₂O (29.6 mg, 0.218 mmol), and ammonium chloride (15.6 mg, 0.292 mmol) in DMF (0.5 mL) were added EDCI (42 mg, 0.218 mmol) and diisopropylethylamine (0.101 mL, 0.58 mmol). The mixture was stirred at ambient temperature overnight and then diluted with EtOAc (10 mL) and H₂O (2.5 mL). The organic layer was separated and evaporated in vacuo to yield the crude amide product. To a solution of the amide product in CH₂Cl₂ (1 mL) was added TFA (0.5 mL), and the resulting mixture was stirred for 3 h. Solvent was removed in vacuo and the residue purified by preparative HPLC (Phenomenex Axia, 8 min gradient, 0–100% B) to give 2q (8.6 mg, 12%) as a white powder. ¹H NMR (400 MHz, CD₃OD) δ 2.76 (s, 3H), 3.88 and 4.12 (AB_q, J = 15.0 Hz, 2H), 4.13 and 4.24 (AB_q, J = 17.2 Hz, 2H), 4.54 (s, 2H), 7.26 (d, J = 8.3 Hz, 1H), 7.45 (dd, J = 8.3, 2.2 Hz, 1H), 7.62 (d, J = 2.2 Hz, 1H). HRMS, Anal. Calcd for C₁₇H₁₇Cl₂N₄O₂: 379.0729. Found: 379.0739 [M + H]⁺. Analytical HPLC: t_R = 3.0 min.

(S)-2-(3-(Aminomethyl)-4-(2,4-dichlorophenyl)-2-methyl-5-oxo-5H-pyrrolo[3,4-*b*]pyridin-6(7H)-yl)-*N,N*-dimethylacetamide (2s). *Procedure A.* To a solution of 18 (100.9 mg, 0.21 mmol) in THF (5.0 mL) was added benzotriazol-1-yloxytripyrrolidinophosphonium hexafluorophosphate (163.9 mg, 0.315 mmol), *N,N*-diisopropylethylamine (0.15 mL, 0.84 mmol), and 2 M NHMe₂/THF (0.157 mL, 0.315 mmol). The reaction mixture was stirred at ambient temperature for 2.5 h and evaporated. The residue was partitioned between EtOAc and H₂O, and the aqueous layer was extracted further with EtOAc (2×). The combined organic extracts were washed with H₂O and brine, dried with (Na₂SO₄), and evaporated under reduced pressure to give the crude amide (186.1 mg) as a light orange solid. The above crude product was dissolved in CH₂Cl₂ (1.5 mL) and treated with TFA (0.8 mL). The reaction mixture was allowed to stir at ambient temperature for 2.5 h and concentrated in vacuo. The residue was purified by preparative HPLC (YMC S5 ODS 30 mm × 100 mm, 12 min gradient, 0–80% solvent B, 40 mL/min) to give 2s, TFA salt (78.9 mg, 98.2% ee, 70% yield over two steps) as an off-white powder. ¹H NMR (500 MHz, CD₃OD) δ 2.83 (s, 3 H), 2.94 (s, 3 H), 3.07 (s, 3 H), 3.95 and 4.19 (AB_q, J = 14.3 Hz, 2 H), 4.39 and 4.51 (AB_q, J = 17.0 Hz, 2 H), 7.33 (d, J = 8.3 Hz, 1 H), 7.51 (d, J = 8.3 Hz, 1 H), 7.69 (s, 1 H). HRMS calculated for C₁₉H₂₁Cl₂N₄O₂: 407.1042. Found: 407.1046 [M + H]⁺.

Procedure B. A mixture of 20 (4.4 g, 7.3 mmol) and 4 N HCl in dioxane (30 mL) was stirred at room temperature for 8.5 h. The reaction mixture was diluted with ether (150 mL) and filtered. The solid cake was washed with ether (150 mL) and dissolved in MeOH (60 mL). The volatiles were removed under reduced pressure to give 2s, dihydrochloride salt, as a beige solid (3.3 g, 86%). The dihydrochloride salt of 2s thus obtained (5.63 g, 11.6 mmol) was dissolved in CH₂Cl₂ (100 mL), and 1 N NaOH (75 mL) was added slowly. The resulting mixture was transferred to a separatory funnel, and the aqueous layer was extracted with CH₂Cl₂ (2 × 100 mL). The combined organic layer was washed with brine, dried (Na₂SO₄), filtered, and concentrated under reduced pressure to afford the free base as a foamy solid. Recrystallization from EtOAc yielded 2s, crystalline free base (4.23 g, 90%), as a colorless solid. Mp 193–194 °C. ¹H NMR (400 MHz, methanol-*d*₄) δ 2.82 (s, 3 H), 2.93 (s, 3 H), 3.06 (s, 3 H), 3.57 and 3.75 (AB_q, J_{AB} = 13.9 Hz, 2 H), 4.39 and 4.48 (AB_q, J_{AB} = 16.8 Hz, 2 H), 4.54 (s, 2 H), 7.33 (d, J = 8.2 Hz, 1 H), 7.45 (dd, J = 8.4, 2.0 Hz, 1 H), 7.61 (d, J = 2.0 Hz, 1 H). ¹³C NMR (125 MHz, CDCl₃) δ 167.34, 166.58, 162.39,

161.22, 143.16, 135.09, 133.70, 133.41, 132.08, 130.80, 129.29, 127.04, 121.22, 51.88, 43.27, 39.83, 36.35, 35.60, 23.04. HRMS calculated for C₁₉H₂₁N₄O₂Cl₂: 407.1042. Found: 407.1041. Elemental analysis calculated: C 55.80, H 4.99, N 13.65, Cl 17.27. Found: C 56.09, H 4.71, N 13.73, Cl 17.40. [α]_D²⁵ +18.8 (c 1.024, MeOH). Analytical HPLC: t_R = 2.6 min.

(S)-2-(3-(Aminomethyl)-4-(2,4-dichlorophenyl)-2-methyl-5-oxo-5H-pyrrolo[3,4-*b*]pyridin-6(7H)-yl)-*N,N*-diethylacetamide, TFA Salt (2n). 59% yield over two steps. ¹H NMR (500 MHz, CD₃OD) δ 1.12 (t, J = 7.2 Hz, 3 H), 1.24 (t, J = 7.2 Hz, 3 H), 2.84 (s, 3 H), 3.34–3.48 (m, 4 H), 3.96 and 4.20 (AB_q, J = 14.3 Hz, 2 H), 4.40 and 4.52 (AB_q, J = 16.7 Hz, 2 H), 4.61 (s, 2 H), 7.34 (d, J = 8.3 Hz, 1 H), 7.51 (d, J = 8.3 Hz, 1 H), 7.69 (s, 1 H). HRMS calculated for C₂₁H₂₅Cl₂N₄O₂: 435.1355. Found: 435.1366 [M + H]⁺.

(S)-2-(3-(Aminomethyl)-4-(2,4-dichlorophenyl)-2-methyl-5-oxo-5H-pyrrolo[3,4-*b*]pyridin-6(7H)-yl)-*N*-methylacetamide, TFA Salt (2r). 74% yield over two steps. ¹H NMR (400 MHz, CD₃OD) δ 2.63 (s, 3 H), 2.74 (s, 3 H), 3.86 and 4.11 (AB_q, J = 14.5 Hz, 2 H), 4.08 and 4.20 (AB_q, J = 16.8 Hz, 2 H), 4.50 (s, 2 H), 7.25 (d, J = 8.3 Hz, 1 H), 7.42 (dd, J = 8.3, 1.6 Hz, 1 H), 7.59 (d, J = 1.6 Hz, 1 H). HRMS calculated for C₁₈H₁₉Cl₂N₄O₂: 393.0885. Found: 393.0894 [M + H]⁺.

(S)-2-(3-(Aminomethyl)-4-(2,4-dichlorophenyl)-2-methyl-5-oxo-5H-pyrrolo[3,4-*b*]pyridin-6(7H)-yl)-*N*-methyl-*N*-propylacetamide, TFA Salt (2t). 57% yield over two steps. ¹H NMR (500 MHz, CD₃OD) δ 0.88 and 0.96 (t, J = 7.3 Hz, 3 H, rotamers), 1.56 and 1.68 (q, J = 7.2 Hz, 2 H, rotamers), 2.84 (s, 3 H), 2.92 and 3.06 (s, 3 H, rotamers), 3.26–3.41 (m, 2 H), 3.96 and 4.20 (AB_q, J = 14.3 Hz, 2 H), 4.33–4.61 (m, 4 H), 7.34 (d, J = 7.7 Hz, 1 H), 7.51 (d, J = 8.3 Hz, 1 H), 7.68 (s, 1H). HRMS calculated for C₂₁H₂₅Cl₂N₄O₂: 435.1355. Found: 435.1368 [M + H]⁺.

(S)-3-(Aminomethyl)-4-(2,4-dichlorophenyl)-2-methyl-6-(2-oxo-2-(pyrrolidin-1-yl)ethyl)-6,7-dihydro-5H-pyrrolo[3,4-*b*]pyridin-5-one, TFA Salt (2u). 45% yield over two steps. ¹H NMR (500 MHz, CD₃OD) δ 1.83–1.95 (m, 2 H), 1.96–2.09 (m, 2 H), 2.84 (s, 3 H), 3.43 (t, J = 6.9 Hz, 2 H), 3.52 (t, J = 6.9 Hz, 2 H), 3.96 and 4.20 (AB_q, J = 14.3 Hz, 2 H), 4.33 and 4.44 (AB_q, J = 17.1 Hz, 2 H), 4.62 (s, 2 H), 7.34 (d, J = 8.3 Hz, 1 H), 7.51 (d, J = 8.3 Hz, 1 H), 7.69 (s, 1 H). HRMS calculated for C₂₁H₂₃Cl₂N₄O₂: 433.1198. Found: 433.1194 [M + H]⁺.

(S)-3-(Aminomethyl)-4-(2,4-dichlorophenyl)-2-methyl-6-(2-oxo-2-(piperidin-1-yl)ethyl)-6,7-dihydro-5H-pyrrolo[3,4-*b*]pyridin-5-one, TFA Salt (2v). 60% yield over two steps. ¹H NMR (500 MHz, CD₃OD) δ 1.55 (m, 2 H), 1.65 (m, J = 24.2, 3.9 Hz, 4 H), 2.84 (s, 3 H), 3.47 (t, J = 5.3, 2H), 3.52 (t, J = 5.0, 2H), 3.96 and 4.20 (AB_q, J = 14.6 Hz, 2 H), 4.41 and 4.50 (AB_q, J = 16.8 Hz, 2 H), 4.59 (s, 2 H), 7.34 (dd, J = 8.3, 2.2 Hz, 1 H), 7.51 (dd, J = 8.3, 1.7 Hz, 1 H), 7.68 (s, 1 H). HRMS calculated for C₂₂H₂₅Cl₂N₄O₂: 447.1355. Found: 447.1362 [M + H]⁺.

In Vitro DPP4 Inhibition Assays. Inhibition of human DPP4 activity was measured under steady-state conditions by following the absorbance increase at 405 nm upon the cleavage of the pseudosubstrate, Gly-Pro-pNA. Assays were performed in 96-well plates using a Thermomax plate reader. Typical reactions contained 100 μ L of ATE buffer (100 mM Aces, 52 mM Tris, 52 mM ethanolamine, pH 7.4), 0.45 nM enzyme, either 120 or 1000 μ M substrate ($S < K_m$ and $S > K_m$, K_m = 180 μ M) and 10 or 11 concentrations of the inhibitor. To ensure steady-state conditions for slow-binding inhibitors, enzyme was preincubated with the compound for 40 min prior to substrate addition. All serial inhibitor dilutions were in DMSO, and final solvent concentration did not exceed 1%. Inhibitor potency was evaluated by calculating IC₅₀ values at each substrate concentration and then converting them to K_i values by assuming competitive inhibition according to the equation $K_i = IC_{50}/[1 + (S/K_m)]$. All inhibitors were competitive as judged by close agreement of K_i values obtained from assays at high and low substrate concentrations. In cases where IC₅₀ at the low substrate concentration was close to the enzyme concentration used in the assay, the data were fit to the Morrison equation to account for the depletion of the free inhibitor.

Oral Glucose Tolerance Test in ob/ob Mice. Male 13- to 14 week-old ob/ob mice (Jackson Labs) were maintained under constant temperature and humidity conditions and a 12 h/12 h light–dark cycle

and had free access to a 10% fat rodent diet (D1245B Research Diets) and tap water. After an overnight fasting period, animals were dosed orally with vehicle (water) or DPP4 inhibitor (0.1–10 $\mu\text{mol/kg}$) at –60 min. Two blood samples were collected at –60 and 0 min by tail bleed for glucose and insulin determinations. Glucose (2 g/kg) was then administered orally (at 0 min). Additional blood samples were collected at 15, 30, 60, 90, and 120 min for glucose and insulin determinations. Blood samples were collected into EDTA containing tubes (Sarstedt). Plasma glucose was determined with an Accu-Chek Advantage (Roche) glucometer. Plasma insulin was assayed using a mouse insulin ELISA kit (ALPCO Diagnostics). Data represent the mean of 12–24 mice/group. Data analysis was performed using one way ANOVA followed by Dunnett's test. All procedures were performed according to BMS-IACUC guidelines.

AUTHOR INFORMATION

Corresponding Author

*Telephone: 609-818-4974. Fax: 609-818-3550. E-mail: pratik.devasthale@bms.com.

Present Address

[∞]L.G.H.: Novartis; e-mail, lawrence.hamann@novartis.com.

[#]R.Z.: PharmD Consulting, LLC; e-mail, bob@rzahler.com.

Notes

The authors declare no competing financial interest.

[×]Deceased.

ACKNOWLEDGMENTS

We thank our colleagues from Discovery Analytical Sciences for their assistance in the characterization of the compounds reported herein, Discovery Synthesis for help with intermediate synthesis at BMS and Syngene, Javed Khan for help with PDB X-ray database depositions, and Fang Moore for help with preparation of the manuscript.

ABBREVIATIONS USED:

hERG EP, human ether-a-go-go related gene; CYP3A4, cytochrome P450 3A4; iv, intravenous; po, per os (oral); oGTT, oral glucose tolerance test; AUC, area under the curve; PDB, Protein Data Bank

REFERENCES

- (1) Recent DPP4 inhibitors reviews: (a) Ahren, B. Emerging Dipeptidyl Peptidase-4 Inhibitors for the Treatment of Diabetes. *Exp. Opin. Emerging Drugs* **2008**, *13* (4), 593–607. (b) Zettl, H.; Schubert-Zsilavecz, M.; Steinhilber, D. Medicinal Chemistry of Incretin Mimetics and DPP-4 Inhibitors. *ChemMedChem* **2010**, *5*, 179–185.
- (2) (a) Dhillon, S. Sitagliptin: A Review of Its Use in the Management of Type 2 Diabetes Mellitus. *Drugs* **2010**, *70* (42), 489–512. (b) Kim, D.; Wang, L.; Beconi, M.; Eiermann, G. J.; Fisher, M. H.; He, H.; Hickey, G. J.; Kowalchick, J. E.; Leiting, B.; Lyon, K.; Marsilio, F.; McCann, M. E.; Patel, R. A.; Petrov, A.; Scapin, G.; Patel, S. B.; Roy, R. S.; Wu, J. K.; Wyvratt, M. J.; Zhang, B. B.; Zhu, L.; Thornberry, N. A.; Weber, A. E. (2R)-4-Oxo-4-[3-(trifluoromethyl)-5,6-dihydro[1,2,4]triazolo[4,3-a]pyrazin-7(8H)-yl]-1-(2,4,5-trifluorophenyl)butan-2-amine: A Potent, Orally Active Dipeptidyl Peptidase IV Inhibitor for the Treatment of Type 2 Diabetes. *J. Med. Chem.* **2005**, *48* (1), 141–151.
- (3) (a) Augeri, D. J.; Robl, J. A.; Betebenner, D. A.; Magnin, D. R.; Khanna, A.; Robertson, J. G.; Wang, A.; Simpkins, L. M.; Taunk, P.; Huang, Q.; Han, S. P.; Abboa-Offei, B.; Cap, M.; Xin, L.; Tao, L.; Tozzo, E.; Welzel, G. E.; Egan, D. M.; Marcinkeviciene, J.; Chang, S. Y.; Biller, S. A.; Kirby, M. S.; Parker, R. A.; Hamann, L. G. Discovery and Preclinical Profile of Saxagliptin (BMS-477118): A Highly Potent, Long-Acting, Orally Active Dipeptidyl Peptidase IV Inhibitor for the Treatment of Type 2 Diabetes. *J. Med. Chem.* **2005**, *48* (15), 5025–5037. (b) Dhillon, S.; Weber, J. Saxagliptin. *Drugs* **2009**, *69* (15), 2103–2114.

- (4) (a) Villhauer, E. B.; Brinkman, J. A.; Naderi, G. B.; Burkey, B. F.; Dunning, B. E.; Prasad, K.; Mangold, B. L.; Russell, M. E.; Hughes, T. E. 1-[[3-(3-Hydroxy-1-adamantyl)amino]acetyl]-2-cyano-(S)-pyrrolidine: A Potent, Selective, and Orally Bioavailable Dipeptidyl Peptidase IV Inhibitor with Antihyperglycemic Properties. *J. Med. Chem.* **2003**, *46* (13), 2774–2789. (b) Banerjee, M.; Younis, N.; Soran, H. Vildagliptin in Clinical Practice: A Review of Literature. *Expert Opin. Pharmacother.* **2009**, *10* (16), 2745–2757.

- (5) Del Prato, S.; Barnett, A. H.; Huisman, H.; Neubacher, D.; Woerle, H.-J.; Dugi, K. A. Effect of Linagliptin Monotherapy on Glycaemic Control and Markers of β -Cell Function in Patients with Inadequately Controlled Type 2 Diabetes: A Randomized Controlled Trial. *Diabetes Obes. Metab.* **2011**, *13*, 258–267.

- (6) (a) Brigrance, R. P.; Meng, W.; Fura, A.; Harrity, T.; Wang, A.; Zahler, R.; Kirby, M. S.; Hamann, L. G. Synthesis and SAR of Azolopyrimidines as Potent and Selective Dipeptidyl Peptidase-4 (DPP4) Inhibitors for Type 2 Diabetes. *Bioorg. Med. Chem. Lett.* **2010**, *20* (15), 4395–4398. (b) Meng, W.; Brigrance, R. P.; Chao, H. J.; Fura, A.; Harrity, T.; Marcinkeviciene, J.; O'Connor, S. P.; Tamura, J. K.; Xie, D.; Zhang, Y.; Klei, H. E.; Weigelt, C. A.; Tuerdi, H.; Wang, A.; Zahler, R.; Kirby, M. S.; Hamann, L. G. Discovery of 6-(Aminomethyl)-5-(2,4-dichlorophenyl)-7-methylimidazo[1,2-a]pyrimidine-2-carboxamides as Potent, Selective Dipeptidyl Peptidase-4 (DPP4) Inhibitors. *J. Med. Chem.* **2010**, *53* (15), 5620–5628. (c) Wang, W.; Devasthale, P.; Wang, A.; Harrity, T.; Egan, D.; Morgan, N.; Cap, M.; Fura, A.; Klei, H. E.; Kish, K.; Weigelt, C. A.; Sun, L.; Levesque, P.; Li, Y.-X.; Zahler, R.; Kirby, M. S.; Hamann, L. G. 7-Oxopyrrolopyridine-Derived DPP4 Inhibitors—Mitigation of CYP and hERG Liabilities via Introduction of Polar Functionalities in the Active Site. *Bioorg. Med. Chem. Lett.* **2011**, *21* (22), 6646–6651. (d) O'Connor, S. P.; Wang, Y.; Simpkins, L. M.; Brigrance, R. P.; Meng, W.; Wang, A.; Kirby, M. S.; Weigelt, C. A.; Hamann, L. G. Synthesis, SAR, and Atropisomerism of Imidazolopyrimidine DPP4 Inhibitors. *Bioorg. Med. Chem. Lett.* **2010**, *20*, 6273–6276. (e) Kirby, M.; Yu, D. M. T.; O'Connor, S. P.; Gorrell, M. D. Inhibitor Selectivity in the Clinical Application of Dipeptidyl Peptidase-4 Inhibition. *Clin. Sci.* **2010**, *118*, 31–41.

- (7) (a) Lankas, G. R.; Leiting, B.; Roy, R. S.; Eiermann, G. J.; Beconi, M. G.; Biftu, T.; Chan, C.-C.; Edmondson, S.; Feeney, W. P.; He, H.; Ippolito, D. E.; Kim, D.; Lyons, K. A.; Ok, H. A.; Patel, R. A.; Petrov, A. N.; Pryor, K. A.; Qian, X.; Reigle, L.; Woods, A.; Wu, J. K.; Zaller, D.; Zhang, X.; Zu, L.; Weber, A. E.; Thornberry, N. A. Dipeptidyl Peptidase IV Inhibition for the Treatment of Type 2 Diabetes. Potential Importance of Selectivity over Dipeptidyl Peptidases 8 and 9. *Diabetes* **2005**, *54*, 2988–2994. (b) Kushner, P.; Gorrell, M. DPP-4 Inhibitors in Type 2 Diabetes: Importance of Selective Enzyme Inhibition and Implications for Clinical Use. *J. Fam. Pract.* **2010**, *59* (2), <http://www.jfponline.com/Pages.asp?AID=8408>. (c) Burkey, B. F.; Hoffmann, P. K.; Hassiepen, U.; Trappe, J.; Juedes, M.; Foley, J. E. Adverse Effects of Dipeptidyl Peptidases 8 and 9 Inhibition in Rodents Revisited. *Diabetes Obes. Metab.* **2008**, *10*, 1057–1061. (d) Wu, J. J.; Tang, H. K.; Yeh, T. K.; Chen, C. M.; Shy, H. S.; Chu, Y. R.; Chien, C. H.; Tsai, T. Y.; Huang, Y. C.; Huang, Y. L.; Huang, C. H.; Tseng, H. Y.; Jiaang, W. T.; Chao, Y. S.; Chen, X. Biochemistry, Pharmacokinetics, and Toxicology of a Potent and Selective DPP8/9 Inhibitor. *Biochem. Pharmacol.* **2009**, *78*, 203–210.

- (8) (a) Peters, J.-U.; Weber, S.; Kritter, S.; Weiss, P.; Wallier, A.; Zimmerli, D.; Boehringer, M.; Steger, M.; Loeffler, B.-M. Amino-methylpyrimidines as DPP-IV Inhibitors. *Bioorg. Med. Chem. Lett.* **2004**, *14*, 3579–3580. (b) Peters, J.-U.; Weber, S.; Kritter, S.; Weiss, P.; Wallier, A.; Boehringer, M.; Hennig, M.; Kuhn, B.; Loeffler, B.-M. Amino-methylpyrimidines as Novel DPP-IV Inhibitors: A 10(5)-Fold Activity Increase by Optimization of Aromatic Substituents. *Bioorg. Med. Chem. Lett.* **2004**, *14*, 1491–1493.

- (9) (a) Sato, Y.; Shimoji, Y.; Fujita, H.; Mizuno, H.; Kumakura, S. Synthetic Studies on Cardiovascular Agents. IV. Synthesis of Fused Dihydropyridine Derivatives (Author's Transl). *Yakugaku Zasshi* **1978**, *98* (4), 448–465. (b) Southwick, P. L.; Barnas, E. F. 4-Benzylidene-2,3-dioxopyrrolidines and 4-Benzyl-2,3-dioxopyrrolidines. Synthesis and Experiments on Reduction and Alkylation. *J. Org. Chem.* **1962**, *27* (1),

98–106. (c) Madhav, R. A New Synthesis of Compounds in the 5*H*-Pyrrolo-[3,4-*b*]pyridine Series. *Synthesis* **1973**, 609–610.

(10) Jang, D. O.; Park, D. J.; Kim, J. A Mild and Efficient Procedure for the Preparation of Acid Chlorides from Carboxylic Acids. *Tetrahedron Lett.* **1999**, *40*, 5323–5326.

(11) Brown, H. C.; Subba Rao, B. C. A New Aldehyde Synthesis. The Reduction of Acid Chlorides by Lithium Tri-*t*-butoxyaluminumhydride. *J. Am. Chem. Soc.* **1958**, *80*, 5377–5380.

(12) (a) X-ray analysis of (*Sa*)-**2s**: PDB deposition number 4JH0. (b) Metzler, W. J.; Yanchunas, J.; Weigelt, C.; Kish, K.; Klei, H. E.; Xie, D.; Zhang, Y.; Corbett, M.; Tamura, J. K.; He, B.; Hamann, L. G.; Kirby, M. S.; Marcinkeviciene, J. *Protein Sci.* **2008**, *17*, 240–250. (c) X-ray analysis of **1e** (BMS-744891)/DPP4 [presumed to be (*Sa*)-**2f**/DPP4]: PDB deposition number 4LKO.

(13) BMS-538305 was used as an internal standard for relevant DPP4-related studies: Simpkins, L. M.; Bolton, S.; Pi, Z.; Sutton, J. C.; Kwon, C.; Zhao, G.; Magnin, D. R.; Augeri, D. J.; Gungor, T.; Rotella, D. P.; Sun, Z.; Liu, Y.; Slusarchyk, W. S.; Marcinkeviciene, J.; Robertson, J. G.; Wang, A.; Robl, J. A.; Atwal, K. S.; Zahler, R. L.; Parker, R. A.; Kirby, M. S.; Hamann, L. G. Potent Non-Nitrile Dipeptidic Dipeptidyl Peptidase IV Inhibitors. *Bioorg. Med. Chem. Lett.* **2007**, *17*, 6476–6480.